University of Alberta

Parameter Estimation and Optimal Detection in Generalized Gaussian Noise

by

Qintian Guo

A thesis submitted to the Faculty of Graduate Studies and Research
in partial fulfillment of the requirements for the degree of

Master of Science

in

Communications

Department of Electrical and Computer Engineering

Abstract

Modern signal processing algorithms need to work in complicated and variable noise environments. The generalized Gaussian distribution (GGD) can be used to accurately model noise in signal processing for telecommunication and other fields because the GGD covers a wide range of distributions. Three distributions widely used for the modeling of noise including the Laplace, Gaussian and uniform distributions are special cases of the GGD with the shape parameter p having values of 1, 2 and ∞ respectively. In this thesis, estimation of the location parameter of the GGD is investigated. When the shape parameter p takes different values, three estimators are derived based on the maximum likelihood estimation theory. An optimal detector in the presence of generalized Gaussian distributed noise is proposed. The asymptotic performance of the optimal detector is analyzed by using the Gaussian approximation method.

Acknowledgements

I would like to give my deepest gratitude to my supervisor, Dr. Norman C. Beaulieu for his continuous support and encouragement during my graduate study. This thesis would not have been possible without his profound knowledge and insightful suggestions. I am also grateful to Dr. Ying Tsui for what he did to help me complete this thesis when Dr. Norman C. Beaulieu is on leave.

I would also like to express my gratitude to my thesis committee for reviewing my thesis.

I am grateful to all my colleagues in the *i*CORE Wireless Communications Laboratory for their friendship and help. Many thanks to Chunxing Jiang, Chuzhe Xiao, Geng Fu, Yanwen Li, Kasun Hemachandra, Payam Dehghani, Samy Botros Soliman, David Young, Navod Suraweera, Ali Sabertali and Mahdi Karami. It is a great honor to be a part of this excellent research team and the training experience in the *i*Core Wireless Communications Laboratory will surely be my lifetime treasure. My special thanks also go to Sijing Jiang, on whose work my M. Sc. thesis is based.

Finally I am extremely grateful to my family for their unconditional love, patience and support. When I was on medical leave for almost one year in 2013, they were always beside me. It is their love that get me through the most difficult time and keep me moving forward.

Contents

List of Figures

List of Symbols

List of Abbreviations

Abbreviation	Description	First use
GGD	Generalized Gaussian distribution	1
UWB	Ultra-wide bandwidth	1
MF	Matched filter	1
PDF	Probability density function	2
BER	Bit error rate	8
ML	Maximum likelihood	8
MSE	Mean square error	8
CRLB	Cramér Rao lower bound	8
i.i.d.	Independent and identically distributed	10
LLF	Log-likelihood function	10
MNS	Moment/Newton-step	15
NL-estimator	Nonlinear estimator	18
L-estimator	Linear estimator	18
CDF	Cumulative distribution function	20
SNR	Signal-to-noise ratio	32
LRT	Log-likelihood ratio test	38
CLT	Central limit theorem	40

Chapter 1

Introduction

1.1 Background

Modern signal processing algorithms need to perform in complicated and variable noise environments. Gaussian background noise model is commonly used for the design of signal processing systems. However, in reality noise sources are often non-Gaussian. The different characters of non-Gaussian noise can significantly degrade the performance of signal processing systems. Accurate statistical model for observed data is important for signal processing applications. Parametric model can be used for generating unknown probability density function of observed data. One parametric model is the generalized Gaussian distribution (GGD). The GGD can be used to accurately model noise in signal processing for telecommunication and many other fields. The GGD covers a wide range of distributions. Three distributions widely used for the modeling of noise including the Laplace, Gaussian and uniform distributions are special cases of the GGD with its shape parameter p having values of 1, 2 and ∞ respectively.

The GGD has been reported to successfully model non-Gaussian noise. For example, it was reported that the generalized Gaussian model is valid for Arctic under-ice noise [1]. Based on samples collected in South China Sea in the winter of 2006, it was concluded that the generalized Gaussian family is suitable for underwater ambient noise [2]. In ultra-wide bandwidth (UWB) receiver structure design, the GGD has been successfully applied to model the probability density function of the multiple access interference in UWB systems [3]. The GGD is also widely used in image coding [4], video coding [5], and speech enhancement [6].

The conventional matched-filter (MF) detector is widely used in receiver design for non-Gaussian noise. The MF detector is optimal for detection in Gaussian noise, yet is suboptimal for detection in non-Gaussian noise. The MF detector significantly degrades the performance of the receiver in presence of generalized Gaussian noise. Therefore it is necessary to find an optimal detector for data detection in generalized Gaussian noise. The minimum error probability principle can be applied to get the optimal detector.

1.2 Generalized Gaussian distribution

The probability density function (PDF) of the GGD is given by [7, 8],

$$f(x) = \frac{1}{2\Gamma(1+1/p)\alpha} \exp\left\{-\left(\frac{|x-\mu|}{\alpha}\right)^p\right\} \tag{1.1a}$$

$$\alpha = \left[\frac{\sigma^2\Gamma(1/p)}{\Gamma(3/p)}\right]^{\frac{1}{2}} \tag{1.1b}$$

where $-\infty < x < \infty$, μ is the location parameter, p is the shape parameter, and σ^2 is the variance. The parameter space is given as,

$$-\infty < \mu < \infty \tag{1.2}$$

$$p > 0 \tag{1.3}$$

$$\alpha > 0 \tag{1.4}$$

$$\sigma^2 > 0. \tag{1.5}$$

The gamma function $\Gamma(\cdot)$ is defined as,

$$\Gamma(t) = \int_0^\infty x^{t-1} \exp(-x) \mathrm{d}x. \tag{1.6}$$

The GGD is more flexible than the Gaussian distribution due to its additional degree of freedom added by the shape parameter p. The GGD becomes the Gaussian distribution when $p = 2$, and becomes sub-Gaussian distributions and super-Gaussian distributions when $p > 2$ and $p < 2$ respectively.

The super-Gaussian distributions with values of p between 0 and 2 represent impulsive noise sources well. When p takes values closer to 0 (more distant from $p = 2$), it becomes more impulsive when the width of the PDF becomes narrower. Fig. 1.1 illustrates the trend of the PDF when p takes values from 2 to 0.5. As shown in Fig. 1.1, the super-Gaussian distributions have sharper peaks around the center and longer tails than the Gaussian distribution. The sub-Gaussian distributions with values of p ranging from $p = 2$ to $p = \infty$ evolve from the Gaussian distribution to the uniform distribution. The trend of the sub-Gaussian PDF is illustrated in Fig. 1.2. As shown in Fig. 1.2, the sub-Gaussian distributions have lower, wider peaks around the center and shorter tails than the Gaussian distribution.

When $p = 1$, the GGD becomes the Laplace distribution,

$$f(x) = \frac{1}{2c} \exp\left\{-\frac{|x-\mu|}{c}\right\} \tag{1.7}$$

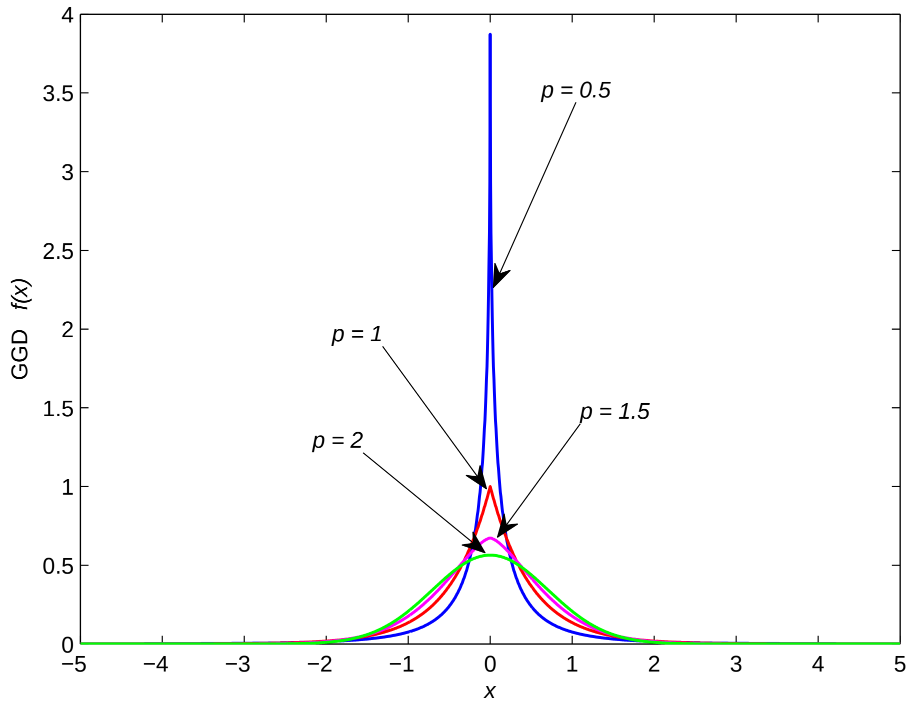

Figure 1.1: The GGD with $p \leq 2$ when the location parameter $\mu = 0$ and the variance σ^2 =1/2.

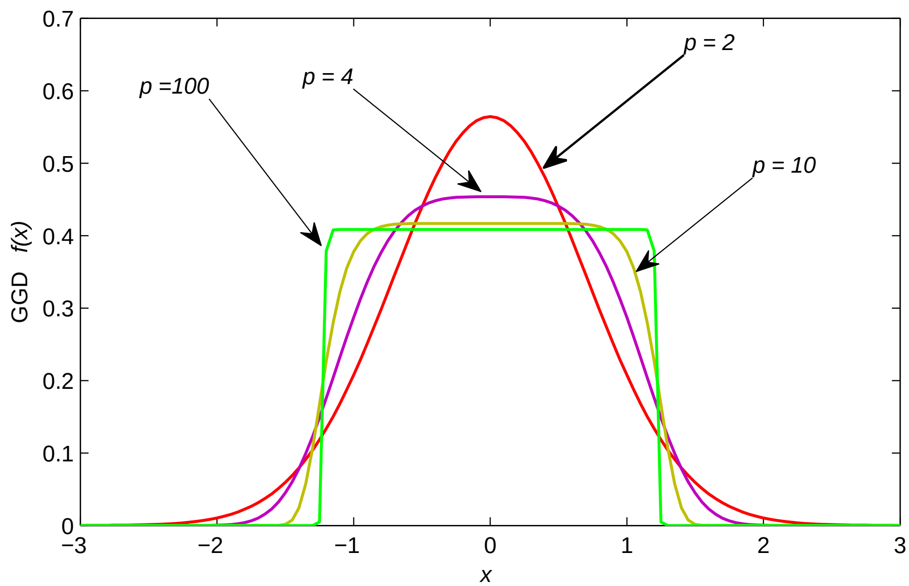

Figure 1.2: The GGD with $p \leq 2$ when the location parameter $\mu = 0$ and the variance σ^2 =1/2.

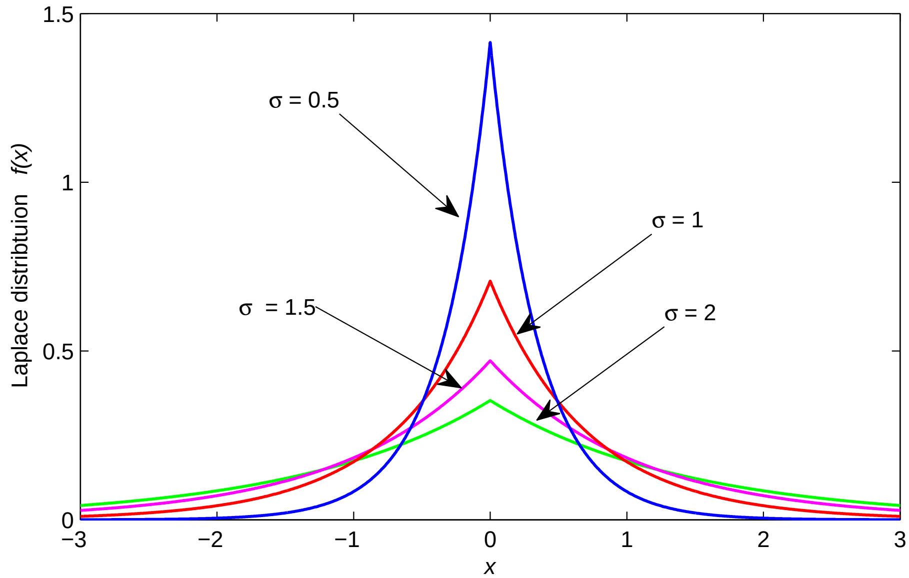

Figure 1.3: The Laplace distribution with different values of the variance σ^2 when the location parameter $\mu = 0$.

where the parameter c is same as α. It is custom to use the letter c instead of α for the Laplace distribution. The relationship of c, α and σ is,

$$c = \alpha = \sqrt{\frac{1}{2}\sigma^2}. \tag{1.8}$$

Fig. 1.3 plots the Laplace distribution when the variance σ^2 takes on different values, illustrating the dependence of the statistical dispersion of the PDF on the variance.

When $p = 2$, the GGD becomes the Gaussian distribution,

$$f(x) = \frac{1}{\sqrt{2\pi\sigma^2}} \exp\left\{-\frac{(x-\mu)^2}{2\sigma^2}\right\}. \tag{1.9}$$

Eq. (1.9) is the PDF of the Gaussian distribution. Fig. 1.4 plots the Gaussian distribution with the variance takes on difference values.

When the shape parameter p approaches to infinity, the GGD becomes the uniform distribution on the interval $[\mu - \alpha, \mu + \alpha]$. The PDF of the uniform distribution can be expressed as,

$$f(x) = \begin{cases} \frac{1}{2\alpha}, & x \in [\mu - \alpha, \mu + \alpha] \\ 0, & \text{otherwise} \end{cases}. \tag{1.10}$$

Fig. 1.5 plots the GGD PDF with $p = 1000$ for several variance values. Even though the shape parameter p is only one thousand, rather than infinity, the PDF of the GGD is close to a uniform distribution.

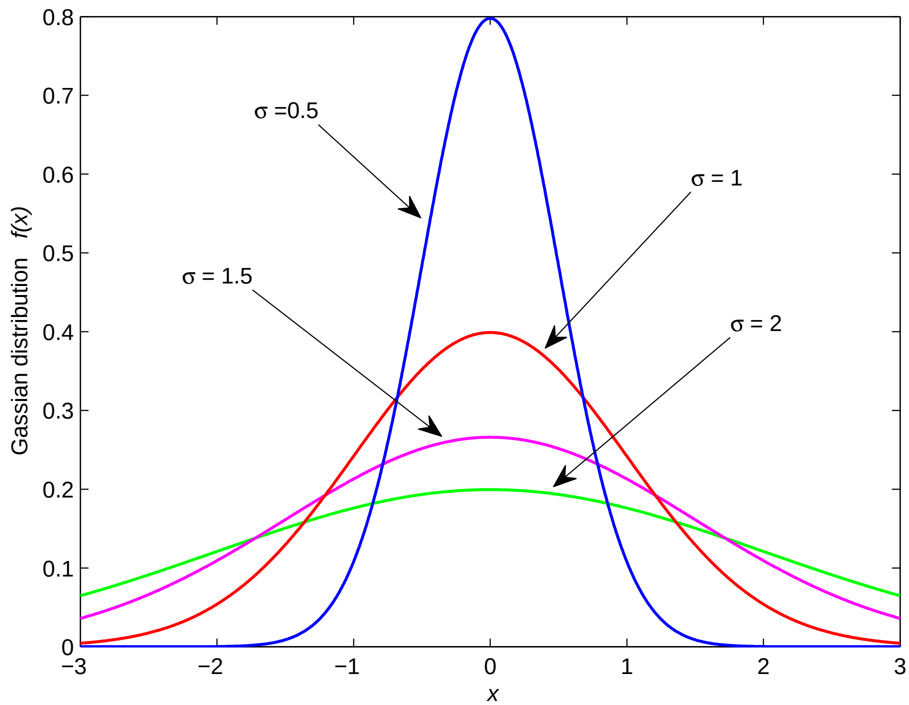

Figure 1.4: The Gaussian distribution with different values of the variance σ^2 when the location parameter $\mu = 0$.

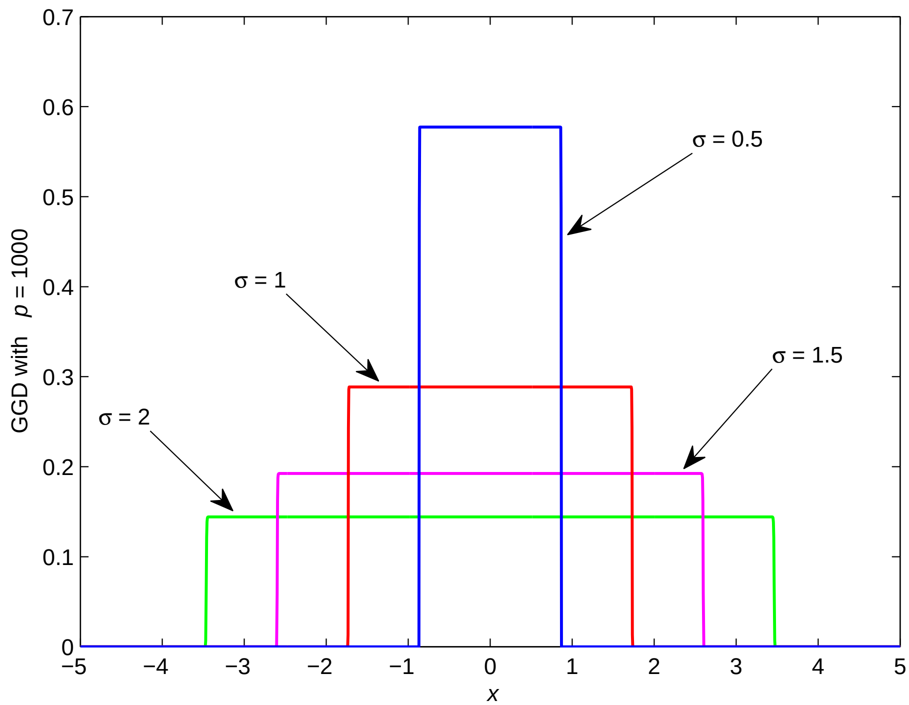

Figure 1.5: The GGD with different values of the variance σ^2 when the location parameter $\mu = 0$ and shape parameter $p = 1000$.

Several mathematical properties of the GGD are provided next.

If X is a random variable of the GGD, then the standardized variable Z can be defined as,

$$Z = \frac{X-\mu}{\alpha}. \tag{1.11}$$

The random variable Z will have the PDF,

$$f(z) = \frac{1}{2\Gamma(1+1/p)} \exp(-|z|^p). \tag{1.12}$$

The kth moment of Z is given by [9],

$$\begin{aligned} E(Z^k) &= \int_{-\infty}^{\infty} z^k \frac{1}{2\Gamma(1+1/p)} \exp(-|z|^p) \mathrm{d}z \\ &= \frac{1+(-1)^k}{2\Gamma(1/p)} \Gamma(\frac{k+1}{p}) \end{aligned} \tag{1.13}$$

where the equation $\Gamma(1+t) = t\Gamma(t)$ was used.

The moments of the random variable Z are used to get the central moments and the moments of the random variable X. The nth central moment of X is given as,

$$\begin{aligned} E\left[(X-\mu)^n\right] &= E\left[\alpha^n Z^n\right] \\ &= \frac{\alpha^n\left[1+(-1)^n\right]}{2\Gamma(1/p)} \Gamma(\frac{n+1}{p}). \end{aligned} \tag{1.14}$$

The nth moment of X can be obtained as,

$$\begin{aligned} E(X^n) &= E\left[(u+\alpha Z)^n\right] \\ &= \frac{\mu^n}{2\Gamma(1/p)} \sum_{k=0}^{n} \binom{n}{k} \left(\frac{\alpha}{\mu}\right)^k \left[1+(-1)^k\right] \Gamma\left[\frac{(k+1)}{p}\right] \end{aligned} \tag{1.15}$$

where $\binom{n}{k}$ denotes combinations of k elements from n elements.

By using the results (1.14) and (1.15), the mean and variance of the random variable X are easily obtained as,

$$E(X) = \mu \tag{1.16}$$

$$Var(X) = \sigma^2. \tag{1.17}$$

1.3 Literature review and research motivation

An optimal detector based on the minimum error probability principle was proposed in [3]. However, no performance analysis of the detector was reported. Analysis of the bit error rate (BER) performance is important for receiver design in presence of generalized Gaussian noise. In this thesis, we analyze the asymptotic BER performance of the optimal detector and provide knowledge of data detection in generalized Gaussian noise.

The implementation of the optimal detector requires knowledge of the received signal amplitude which needs to be estimated at the receiver before data detection in order to optimize the performance of the receiver. Estimation of the received signal amplitude in generalized Gaussian noise can be regarded as estimation of the location parameter of the GGD.

In literature, the estimators currently adopted are the mean estimator and the median estimator. In [10], for $p \leq 2$, the sample mean and sample median have good performance in estimating the location parameter of the GGD. When p increases from 2, the performance of these two estimators degrades significantly and they prevent receivers with the optimal detector from achieving their optimal performance. By assuming that the shape parameter is known, the maximum likelihood (ML) estimation equation of the location parameter could be easily obtained. Though the ML estimator has optimal performance, in general there is no closed-form expression for the ML estimator. Therefore, to implement the optimal detector, it is necessary to give efficient estimators for the location parameter.

1.4 Contributions

This thesis mainly focuses on parameter estimation and optimal detection in Generalized Gaussian noise.

In Chapter 2, three estimators are proposed based on the ML estimation theory. They enhance our knowledge of estimation of the location parameter of the GGD. The first estimator is an exact ML estimator for $p = 4$. It is an optimal design and gives an explicit closed-form expression whereas previous estimators for $p = 4$ were based on numerical solutions of the ML equation. The second estimator is a non-linear estimator for $p \geq 2$, which has a simple structure and excellent mean square error (MSE) performance. The non-linear estimator is unbiased and compatible with known superior estimators. A generalized non-linear estimator is also mentioned. Finally, the third estimator, an approximate ML estimator for $p = 5$ is proposed. In terms of MSE performance, the proposed approximate ML estimator gives better performance than previous best estimators. These works have been published in the *IEEE Communications Letters* and *IEEE Signal Processing Letters* [11 - 13]. A close-form expression for the Cramér Rao lower bound (CRLB) is derived as well.

In Chapter 3, an optimal detector for generalized Gaussian distributed noise is proposed based on the minimum error probability decision rule. The asymptotic BER performance of the optimal detector is analyzed by using the Gaussian approximation method. A closed-form expression for the asymptotic BER performance is obtained and numerical simulations are done to verify the theoretical result.

1.5 Outline of thesis

This chapter introduced the motivation and background of the thesis. Some common properties of the GGD were also discussed. The moments and central moments of the GGD as well as some integrals that will be used in Chapter 3 were also derived in this chapter.

Chapter 2 focuses on the estimation problem of the location parameter for the GGD. The ML estimation equation is derived first, and then the CRLB for estimators for the location parameter is discussed. Three new estimators are derived and numerical results are given to show the performances of the proposed estimators.

In Chapter 3, an optimal detector in the presence of generalized Gaussian distributed noise first, and then using the Gaussian approximation method, the asymptotic BER performance of the optimal detector is analyzed. A closed-form expression for the asymptotic performance is obtained. Simulations in a special case of half-sine pulse shape are performed to verify the theoretical analysis.

Finally, Chapter 4 concludes the thesis and suggests some potential future research directions.

Chapter 2

Estimators for the location parameter of the GGD

2.1 ML estimation

In Page 2, the probability density function (PDF) of the GGD has been introduced. Let us write the expression here again,

$$f(x) = \frac{1}{2\Gamma(1+1/p)\alpha} \exp\left\{-\left(\frac{|x-\mu|}{\alpha}\right)^p\right\} \tag{1.1a}$$

$$\alpha = \left[\frac{\sigma^2\Gamma(1/p)}{\Gamma(3/p)}\right]^{\frac{1}{2}}. \tag{1.1b}$$

In this thesis, when studying the problem of estimation, we focus on estimating the location parameter μ. we assume that the shape parameter p has been known or estimated.[1]

Let $X_1, X_2, ..., X_n$ be independent and identically distributed (i.i.d.) random samples from a GGD. Define a vector $\bar{X} = [X_1, X_2, ..., X_n]$. Thus, the multivariate generalized Gaussian distributed PDF is

$$f(\bar{x}|\mu) = \prod_{i=1}^{n} \frac{1}{2\Gamma(1+1/p)\alpha} \exp\left\{-\left(\frac{|x_i-\mu|}{\alpha}\right)^p\right\}. \tag{2.2}$$

Here the log-likelihood function (LLF) with n samples is,

$$\ln f(\bar{x}|\mu) = -n\ln[2\Gamma(1+1/p)\alpha] - \sum_{i=1}^{n} \frac{|x_i-\mu|^p}{\alpha^p}. \tag{2.3}$$

According to the ML principle, taking the derivative of (2.3) with respect to μ and setting the result equal to zero, the ML estimation equation is obtained,

$$\sum_{i=1}^{n} \text{sgn}(x_i-\mu)|x_i-\mu|^{p-1} = 0 \tag{2.4}$$

[1] If estimation of p needs knowledge of the location parameter μ, we can use the average of the samples as μ. The estimated p may have small deviation from the true value. However, since the NL-estimator proposed in Section 2.4 is robust, we can use the estimated p to estimate μ and get a much exacter estimated μ. An exacter estimated μ gives an exacter estimated p.

where x_i are known variables , μ is unknown and sgn denotes the signum function given as [14],

$$\operatorname{sgn}(x) = \begin{cases} 1, & x > 0 \\ 0, & x = 0 \; . \\ -1, & x < 0 \end{cases} \tag{2.5}$$

The ML estimator for the GGD is given by the solution of (2.4).

Unfortunately, no explicit solution of (2.4) is available for arbitrary p. The only exceptions are $p = 1$, p= 2 and $p = \infty$ for which the GGD becomes the Laplace distribution, the Gaussian distribution and the uniform distribution, respectively.

In the case of the Laplace distribution, namely $p = 1$, the ML estimation equation (2.4) becomes,

$$\sum_{i=1}^{n} \operatorname{sgn}(x_i - \mu) = 0. \tag{2.6}$$

The solution of (2.6) is given as the median [15],

$$\hat{\mu} = \operatorname{median}(x_i) = \begin{cases} z_{\frac{n+1}{2}}, & n = 2k+1 \\ \\ \frac{z_{\frac{n}{2}} + z_{\frac{n}{2}+1}}{2}, & n = 2k \end{cases} . \tag{2.7}$$

where the order statistics of $\{X_i\}_{i=1}^{n}$ are defined as $\{Z_i\}_{i=1}^{n}$, and $Z_1 \leq Z_2 \leq ... \leq Z_n$. In the case of the Gaussian distribution, namely $p = 2$, the ML estimation equation (2.4) becomes,

$$\sum_{i=1}^{n} (x_i - \mu) = 0. \tag{2.8}$$

So the solution of (2.8) is given as the mean,

$$\hat{\mu} = \operatorname{mean}(x_i) = \frac{\sum_{i=1}^{n} x_i}{n}. \tag{2.9}$$

In the case of the uniform distribution, namely $p = \infty$, the solution of the ML estimation equation (2.4) is given as the midrange [16],

$$\hat{\mu} = \operatorname{midrange}(x_i) = \frac{\max(x_i) + \min(x_i)}{2} \tag{2.10}$$

where $\max(x_i)$ is the maximum of the random samples x_i and $\min(x_i)$ is the minimum of the random samples x_i.

2.2 Cramér Rao lower bound

In this section, the Cramér Rao lower bound (CRLB) is derived. The ML estimator for the location parameter of the GGD is unbiased [17]. The variance of any unbiased estimator is bounded by the CRLB [18, Theorem 3.1].

The Cramér Rao lower bound (CRLB) is given as the inverse of the Fisher information $I(\mu)$,

$$\text{CRLB} = \frac{1}{I(\mu)} \tag{2.11a}$$

and the Fisher information is defined as,

$$I(\mu) = -E[\frac{\partial^2}{\partial \mu^2} \ln f(\bar{x}|\mu)] \tag{2.11b}$$

where the notation $E(\cdot)$ denotes expectation operation.

For a single observation, the second-order derivatives of the LLF is given in [9],

$$\frac{\partial^2}{\partial \mu^2} \ln f(x_i|\mu) = -\frac{p(p-1)}{\alpha^2} \left| \frac{(x_i - \mu)}{\alpha} \right|^{p-2}. \tag{2.12}$$

When p is even, the expectation of $\left|\frac{(x_i-\mu)}{\alpha}\right|^{p-2}$ is,

$$E\left[\left|\frac{(x_i - \mu)}{\alpha}\right|^{p-2}\right] = E\left[\left(\frac{x_i - \mu}{\alpha}\right)^{p-2}\right]$$

$$= \frac{1}{\Gamma(1/p)}\Gamma(1 - 1/p). \tag{2.13}$$

When p is odd, the expectation of $\left|\frac{(x_i-\mu)}{\alpha}\right|^{p-2}$ is,

$$E\left[\left|\frac{(x_i - \mu)}{\alpha}\right|^{p-2}\right]$$

$$= \int_{-\infty}^{\mu} -\left(\frac{x - \mu}{\alpha}\right)^{p-2} f(x)\mathrm{d}x + \int_{\mu}^{\infty} \left(\frac{x - \mu}{\alpha}\right)^{p-2} f(x)\mathrm{d}x$$

$$= \frac{-(-1)^{p-2}}{2\Gamma(1/p)}\Gamma\left(\frac{p-1}{p}\right) + \frac{1}{2\Gamma(1/p)}\Gamma\left(\frac{p-1}{p}\right)$$

$$= \frac{1}{\Gamma(1/p)}\Gamma(1 - 1/p). \tag{2.14}$$

Therefore, when p is an integer, the expectation of (2.12) is given by

$$E[\frac{\partial^2}{\partial\mu^2}\ln f(x_i|\mu)]$$

$$= -\frac{p(p-1)}{\alpha^2}\frac{1}{\Gamma(1/p)}\Gamma(1-1/p)$$

$$= -\frac{p^2\Gamma(2-1/p)}{\alpha^2\Gamma(1/p)} \tag{2.15}$$

Since $X_1, X_2, ..., X_n$ are i.i.d. random samples, the Fisher information $I(\mu)$ is given as,

$$\begin{aligned} I(\mu) &= -E[\frac{\partial^2}{\partial\mu^2}\ln f(\bar{x}|\mu)] \\ &= -\sum_{i=1}^{n} E[\frac{\partial^2}{\partial\mu^2}\ln f(x_i|\mu)] \\ &= \frac{np^2\Gamma(2-1/p)}{\alpha^2\Gamma(1/p)}. \end{aligned} \tag{2.16}$$

Using (2.11a) and (2.16), a compact closed-form expression for the CRLB is derived, that is

$$\text{CRLB} = \frac{\alpha^2\Gamma(1/p)}{np^2\Gamma(2-1/p)} \tag{2.17}$$

where p is an integer.

Though (2.17) was derived in the case of integer p, simulations show that it is applicable for non-integer p. Since the variable x in $\Gamma(x)$ should not be negative integers or zero, p should satisfy $p \neq 1/k$, where k is an integer greater than 1.

2.3 True ML estimator for $p = 4$

An explicit solution for the GGD with $p = 4$ is derived in this section.[2]

2.3.1 True ML estimator for $p = 4$

In Section 2.1, ML estimation of the location parameter of the GGD has been introduced. Let $X_1, X_2, ..., X_n$ be independent and identically distributed (i.i.d.) random samples from a GGD with (μ, p, σ^2). Define a vector $\bar{X} = [X_1, X_2, ..., X_n]$. The ML estimation equation is given in (2.4), which is,

$$\sum_{i=1}^{n} \mathrm{sgn}(x_i - \mu)|x_i - \mu|^{p-1} = 0. \tag{2.4}$$

There are only three values of p for which the true ML estimator is known in an explicit form. They are $p = 1$, $p = 2$ and $p = \infty$. In this section, a new exact ML estimator for $p = 4$ is derived. The process of derivation of the new estimator is given as following.

When the shape parameter $p = 4$, eq. (2.4) becomes,

$$\sum_{i=1}^{n} (x_i - \mu)^3 = 0. \tag{2.18}$$

Expand the above equation by using binomial expansion,

$$n \cdot \mu^3 - 3\sum_{i=1}^{n} x_i \cdot \mu^2 + 3\sum_{i=1}^{n} {x_i}^2 \cdot \mu - \sum_{i=1}^{n} {x_i}^3 = 0 \tag{2.19}$$

where the variables x_i are known and the location parameter μ is unknown deterministic. Eq. (2.19) is a cubic equation in μ. Corresponding to the general form of a cubic equation, $\mu^3 + a\mu^2 + b\mu^2 + c = 0$, each coefficient is given as,

$$a = -\frac{3\sum_{i=1}^{n} x_i}{n} \tag{2.20a}$$

$$b = \frac{3\sum_{i=1}^{n} {x_i}^2}{n} \tag{2.20b}$$

$$c = -\frac{\sum_{i=1}^{n} {x_i}^3}{n}. \tag{2.20c}$$

Three intermediate variables are defined below to express the roots of a cubic equation,

$$s = \frac{(3b - a^2)}{3} \tag{2.21a}$$

$$t = \frac{2a^3 - 9ab + 27c}{27} \tag{2.21b}$$

$$\Delta = -4s^3 - 27t^2 \tag{2.21c}$$

[2] The work in this section has been published in *IEEE Communications Letters* [12].

where Δ in (2.21c) is the discriminant of the cubic equation. For a cubic equation with real coefficients, if $\Delta > 0$, the equation has three distinct real roots; if $\Delta < 0$, the equation has one real root and two complex conjugate roots; if $\Delta = 0$, the equation has a double real root and a simple real root, or a triple real root [19]. Eq. (2.4) has a unique real solution in probability for $p > 1$ [7]. The unique real root of (2.19) is given by [20, p. 23],

$$\hat{\mu} = -\frac{a}{3} + \frac{1}{3}\sqrt[3]{-\frac{27}{2}t + \frac{3}{2}\sqrt{-3\Delta}} - \frac{s}{\sqrt[3]{-\frac{27}{2}t + \frac{3}{2}\sqrt{-3\Delta}}}. \tag{2.21d}$$

Eq. (2.21d) is an explicit closed-form expression for the ML estimator obtained for the GGD with $p = 4$.

It is an incremental contribution for the following reasons.

1. It is an optimal design.

2. The range of values of p extends from 0 to infinity and there is a fundamental and natural division of the range of p into two ranges 0 to 2, and 2 to infinity. The optimal estimator for the upper endpoint of the $p = 2$ to infinity range, i.e., infinity, is known. Finding the optimal estimator for $p = 4$, sets a new and improved limit on the range for which optimal estimators are known, i.e., the improvement is in changing the range from 2 to infinity to 4 to infinity. This reduces the range for which optimal estimators for the GGD are not known.

3. The optimal estimator for $p = 4$ is given in an explicit form whereas previous estimators for this value were based on numerical solutions of the ML equation.

2.3.2 Numerical results and discussion

In this subsection, we compare the mean square error (MSE) of the proposed ML estimator with the MSEs of the mean estimator and the moment/Newton-step (MNS) estimator [7] as well as with the Cramér Rao lower bound (CRLB).

The mean estimator, rather than the median estimator, is chosen for comparison. Recall that the median estimator is the ML estimator for $p = 1$, and the mean estimator is the ML estimator for $p = 2$. It is intuitive that the median estimator will become increasingly worse compared to the mean estimator as p increases to 4. Simulations verify this behaviour.

The MNS estimator proposed in [7] is a corollary of Newton's method [21]. Newton's method is a useful iterative method for seeking the roots of a real-value function [22]. Therefore the MNS estimator should be regarded as an approximate ML estimator. An explicit expression for the MNS estimator is given as,

$$\hat{\mu}_{mns} = \mu_0 + \frac{\Gamma(1/p)}{np\alpha^{p-2}\Gamma(2-1/p)} \cdot \sum_{i=1}^{n} sgn(x_i - \mu_0)|x_i - \mu_0|^{p-1} \tag{2.22}$$

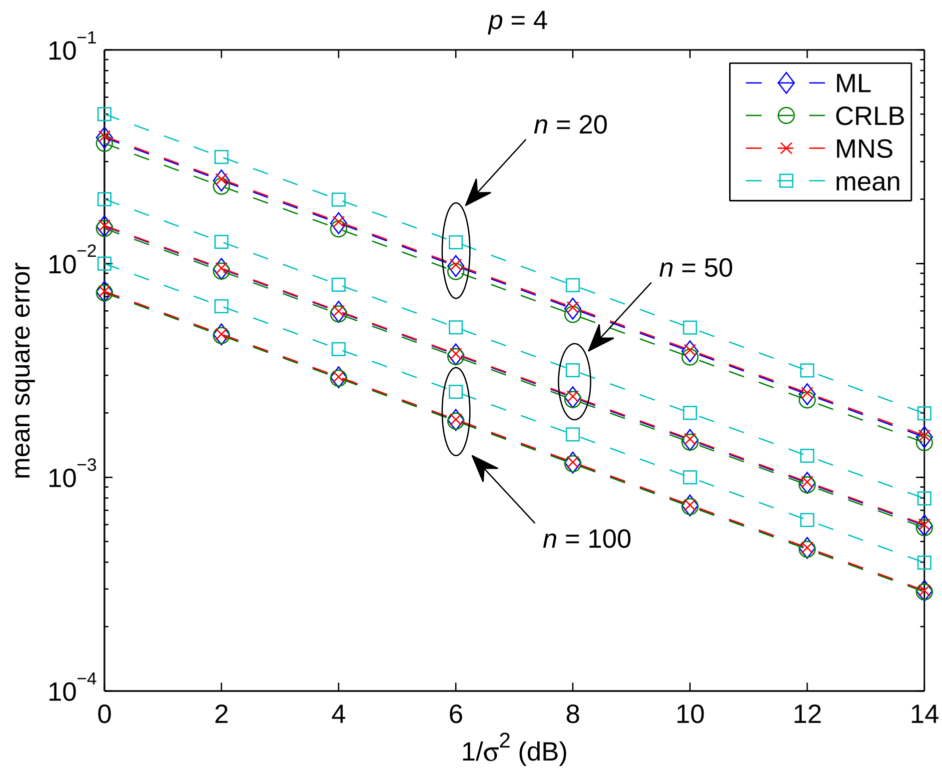

Figure 2.1: The MSEs of the ML estimator, the MNS estimator and the mean estimator and the CRLB with $p = 4$.

where p is equal to 4 in this section and μ_0 takes the value of the mean estimator.

The ML estimator for the location parameter of the GGD is unbiased [17]. The variance of any unbiased estimator is bounded by the CRLB [18, Theorem 3.1]. The CRLB for the GGD was derived in Section 2.2; it is

$$Var[\hat{\mu}] \geq \text{CRLB} = \frac{\sigma^2}{12n}\left(\frac{\Gamma(1/4)}{\Gamma(3/4)}\right)^2. \tag{2.23}$$

The mean estimator is also unbiased and its variance (equal to its MSE) is given as,

$$E[(\hat{\mu}_{mean} - \mu)^2] = \frac{\sigma^2}{n}. \tag{2.24}$$

We fix the location parameter of the GGD $\mu = 1$ and give $1/\sigma^2$ values between 0 dB and 14 dB. The MSEs of the estimators are obtained by using Monte Carlo simulation. The number of trials used for estimating the MSEs in Fig. 2.1 is five million.

Fig. 2.1 compares the MSE of the new ML estimator with the CRLB. When $n = 20$, the MSE of the ML estimator has a small disadvantage of about 0.26 dB over the CRLB; when $n = 50$, the gap between the MSE of the ML estimator and the CRLB decreases to about 0.1 dB; When $n = 100$, the gap further decreases to about 0.05 dB and the two curves for the ML estimator and the CRLB are graphically coincident. Note that as n increases, the MSE of the ML estimator becomes closer to the CRLB. The ML estimator is asymptotically efficient for $p = 4$ [7].

Fig. 2.1 also shows the MSEs of the MNS estimator and the mean estimator. For $n = 20$, the MSE loss of the MNS estimator relative to the ML estimator is 0.065 dB, and the MSE loss of the mean estimator relative to the ML estimator is 1.11 dB. When $n = 50$ and $n = 100$, the MSE gaps between the ML estimator and the MNS estimator decrease to 0.033 dB and 0.018 dB, respectively, while the MSE gaps between the ML estimator and the mean estimator increase to 1.26 dB and 1.31 dB, respectively. Obviously the mean estimator gives increasingly worse performance as the sample size n increases. As n tends to ∞, the theoretical MSE gap between the ML estimator and the mean estimator is equal to $12\left(\frac{\Gamma(3/4)}{\Gamma(1/4)}\right)^2 \approx 1.3708$ dB. It is also concluded that as the sample size n increases, the MNS estimator gives increasingly better performance. However, it remains a fact that the ML estimator is exact and the MNS estimator is approximate.

2.3.3 Summary

Heretofore, explicit solutions for the ML estimator of the location parameter of the GGD were only known for values of parameter, $p = 1$, $p = 2$, and $p = \infty$. For $p = 1$ the GGD becomes the Laplace distribution, and the sample median is the ML estimator. For $p = 2$ the GGD becomes the Gaussian distribution, and the sample mean is the ML estimator. For $p = \infty$, the GGD becomes the uniform distribution, and the extreme two-sample midpoint is the ML estimator. An explicit solution for the case of $p = 4$ was derived in this section. Reporting an explicit form for the ML estimator for $p = 4$ is an incremental contribution.

The MSE of the ML estimator for $p = 4$ was compared to the CRLB. The ML estimator has practical value as it attains the CRLB at moderate sample size. The MSE was also compared to the MSE of the mean estimator and it was found that the ML estimator greatly outperforms the mean estimator. The ML estimator has slight advantage compared to the MNS estimator.

2.4 NL-estimator

A new unbiased estimator, named as the NL-estimator[3], is proposed in this section for $p \in [2, \infty)$.[4]

2.4.1 NL-estimator

Let $X_1, X_2, ..., X_n$ be independent and identically distributed (i.i.d.) random samples from a GGD with parameters $(\mu,\ p,\ \sigma^2)$. The ML estimation equation is given in (2.4), which is,

$$\sum_{i=1}^{n} \operatorname{sgn}(x_i - \mu)|x_i - \mu|^{p-1} = 0. \tag{2.4}$$

In seeking an improved estimator for the GGD, we note that when $p = \infty$ the GGD becomes the uniform distribution and the ML estimator is the midpoint of the first and last order statistics. For other values of p, this estimator is wasteful of the other samples as it discards them. This thinking leads us to assume an estimator structure which starts by computing the midpoint of the ith and $(n - i + 1)$th order statistics, and then combines these midpoint estimators by some weighting (reliability) scheme.

Some variables are now defined that are needed in the sequel. Define new random variables $\{Z_i\}_{i=1}^n$ as the order statistics corresponding to $\{X_i\}_{i=1}^n$, where $Z_1 \leq Z_2 \leq ... \leq Z_n$. The midpoint $\hat{\mu}_i$ and the range R_i of the sample pair (z_i, z_{n-i+1}) are respectively given as,

$$\hat{\mu}_i = \frac{z_{n-i+1} + z_i}{2} \tag{2.25}$$

$$R_i = z_{n-i+1} - z_i. \tag{2.26}$$

Heuristically, noting that the argument of the exponential function in the PDF in (1.1) involves a power function of x, we apply a power weighting of the range of the ith ranked midpoint estimator, and select as an estimator design,

$$\hat{\mu} = \sum_{i=1}^{\frac{n}{2}} \alpha_i \cdot \hat{\mu}_i \tag{2.27a}$$

$$\alpha_i = \frac{{R_i}^m}{\sum_{j=1}^{\frac{n}{2}} {R_j}^m}, \qquad i = 1, 2, ..., \frac{n}{2} \tag{2.27b}$$

where the sample size n is assumed to be even. The estimator structure in (2.27) admits a degree of freedom through the choice of m. Simulations show $m = p - 2$ is

[3]The name, NL-estimator was used in [11] to distinguish the L-estimator which is a linear combination of order statistics.

[4]The work in this section has been published in part in *IEEE Communications Letters* [11].

a good choice. Simulation results show that in the case when p is non-integer, the new estimator (2.27) with $m = p - 2$ still gives excellent performance. Therefore the new estimator (2.27) can be used for $p \in [2, \infty)$.

In contrast to L-estimators which are linear combinations of the order statistics [23], this novel estimator forms a weighted non-linear sum of the order statistics; we shall call this estimator the NL-estimator.

The NL-estimator is compatible with known superior estimators. Note that the GGD with $p = 2$ yields the Gaussian distribution. For $p = 2$,

$$\alpha_i = \frac{2}{n}, \qquad i = 2, ..., \frac{n}{2} \tag{2.28}$$

$$\hat{\mu}_{NL} = \frac{1}{n}\sum_{i=1}^{n} z_i \tag{2.29}$$

and the NL-estimator simplifies to the mean estimator, which is the ML estimator for the Gaussian distribution.

When $p = \infty$, the GGD yields the uniform distribution, and as a result,

$$\lim_{p\to\infty} \alpha_1 = \lim_{p\to\infty} \frac{(z_n - z_1)^{p-2}}{\sum_{i=1}^{\frac{n}{2}} (z_{n-i+1} - z_i)^{p-2}} = 1 \tag{2.30}$$

$$\lim_{p\to\infty} \alpha_i = 0, \qquad i = 2, ..., \frac{n}{2} \tag{2.31}$$

$$\lim_{p\to\infty} \hat{\mu}_{NL} = \frac{(z_n + z_1)}{2} = \text{midrange}. \tag{2.32}$$

The unbiased ML estimator for the midpoint of the uniform distribution is the midrange estimator given in (2.32) [16].

Finally the NL-estimator can be adjusted for the case when the sample size is odd, by discarding the sample median. Our simulations indicate that negligible effect on the estimator performance results from doing so. The final, simple form of the new estimator is then given as,

$$\hat{\mu}_{NL} = \sum_{i=1}^{\frac{n_e}{2}} \alpha_i \cdot \hat{\mu}_i \tag{2.33}$$

$$\alpha_i = \frac{{R_i}^{p-2}}{\sum_{j=1}^{\frac{n_e}{2}} {R_j}^{p-2}} \tag{2.34}$$

$$\hat{\mu}_i = \frac{z_i + z_{n-i+1}}{2} \tag{2.35}$$

$$R_i = z_{n-i+1} - z_i \tag{2.36}$$

$$n_e = \begin{cases} n, & n \text{ even} \\ n-1, & n \text{ odd} \end{cases}. \tag{2.37}$$

The statistic $\hat{\mu}_i$ is proved to be an unbiased estimator for the location parameter.
Proof. Let $X_1, X_2, ..., X_n$ be i.i.d. random samples from a GGD. Let $Z_1 \leq Z_2 \leq ... \leq Z_n$ be the corresponding order statistics of $X_1, X_2, ..., X_n$. Let $f(\cdot)$ and $F(\cdot)$ denote the PDF and the cumulative distribution function (CDF) of each sample, respectively. The PDF of Z_i is given by [16, p. 254],

$$f_{Z_i}(z) = \frac{n!}{(i-1)!(n-i)!}[F(z)]^{i-1}[1-F(z)]^{n-i}f(z) \tag{2.38}$$

where the factorial of a non-negative integer n is denoted as $n!$. The midpoint estimator $\hat{\mu}_i$ is given in (2.25) and the expectation of $\hat{\mu}_i$ is given as,

$$E(\hat{\mu}_i) = \frac{E(z_{n-i+1}) + E(z_i)}{2}. \tag{2.39}$$

Using (2.38), the expectations of z_{n-i+1} and z_i are respectively derived as

$$\begin{aligned} E(z_{n-i+1}) &= \int_{-\infty}^{\infty} z \cdot f_{Z_{n-i+1}}(z)dz \\ &= \int_{-\infty}^{\infty} z \cdot c \cdot [F(z)]^{n-i}[1-F(z)]^{i-1}f(z)dz \\ &= \int_{0}^{1} F^{-1}(1-v) \cdot c \cdot v^{i-1}(1-v)^{n-i}dv \end{aligned} \tag{2.40a}$$

$$\begin{aligned} E(z_i) &= \int_{-\infty}^{\infty} z \cdot f_{Z_i}(z)dz \\ &= \int_{-\infty}^{\infty} z \cdot c \cdot [F(z)]^{i-1}[1-F(z)]^{n-i}f(z)dz \\ &= \int_{0}^{1} F^{-1}(w) \cdot c \cdot w^{i-1}(1-w)^{n-i}dw \end{aligned} \tag{2.40b}$$

where $F^{-1}(\cdot)$ is the inverse function of $F(\cdot)$ and

$$c = \frac{n!}{(n-i)!(i-1)!} \tag{2.41}$$

$$v = 1 - F(z) \tag{2.42}$$

$$w = F(z). \tag{2.43}$$

The inverse function of $F(\cdot)$ exists because the PDF $f(\cdot)$ satisfies $f(x) > 0$ for all $x \in (-\infty, \infty)$.

Note that the PDF $f(\cdot)$ of the GGD is symmetric about μ. Thus for arbitrary $y \in (0, 1)$,

$$F^{-1}(1-y) + F^{-1}(y) = 2 \cdot \mu \tag{2.44}$$

where μ is the location parameter of the GGD.

Substituting (2.40) and (2.44) into (2.39), we obtain

$$\begin{aligned} E(\hat{\mu}_i) &= \frac{E(z_{n-i+1}) + E(z_i)}{2} \\ &= \int_0^1 \frac{F^{-1}(y) + F^{-1}(1-y)}{2} \cdot c \cdot y^{i-1}(1-y)^{n-i} dy \\ &= \mu \cdot \int_0^1 c \cdot y^{i-1}(1-y)^{n-i} dy \\ &= \mu \end{aligned} \tag{2.45}$$

where we use the equation,

$$1 = \int_{-\infty}^{\infty} f_{Z_i}(z) dz = \int_0^1 c \cdot y^{i-1}(1-y)^{n-i} dy \tag{2.46}$$

and the proof is complete.

The statistics $\hat{\mu}_i$ are unbiased estimators and the equation $\sum_{i=1}^{\frac{n}{2}} \alpha_i = 1$ yield that the NL-estimator is unbiased.

2.4.2 Numerical results and discussion

In this subsection, numerical results are given to show the performance of the proposed NL-estimator.

We compare the NL-estimator with the ML estimator and the mean estimator. All these estimators are unbiased. Note that since the estimators are unbiased, the MSE is equal to the estimator variance and no residual bias is included in the MSE. The MSE estimated by Monte Carlo simulation is used to evaluate their performances. We set the location parameter $\mu = 1$ and give $\frac{1}{\sigma^2}$ values between 0 dB and 10 dB.

Fig. 2.2 compares the MSEs of the NL-estimator, the ML estimator, the mean estimator and the median estimator with $p = 4$. When $n = 50$, there is a 1.27

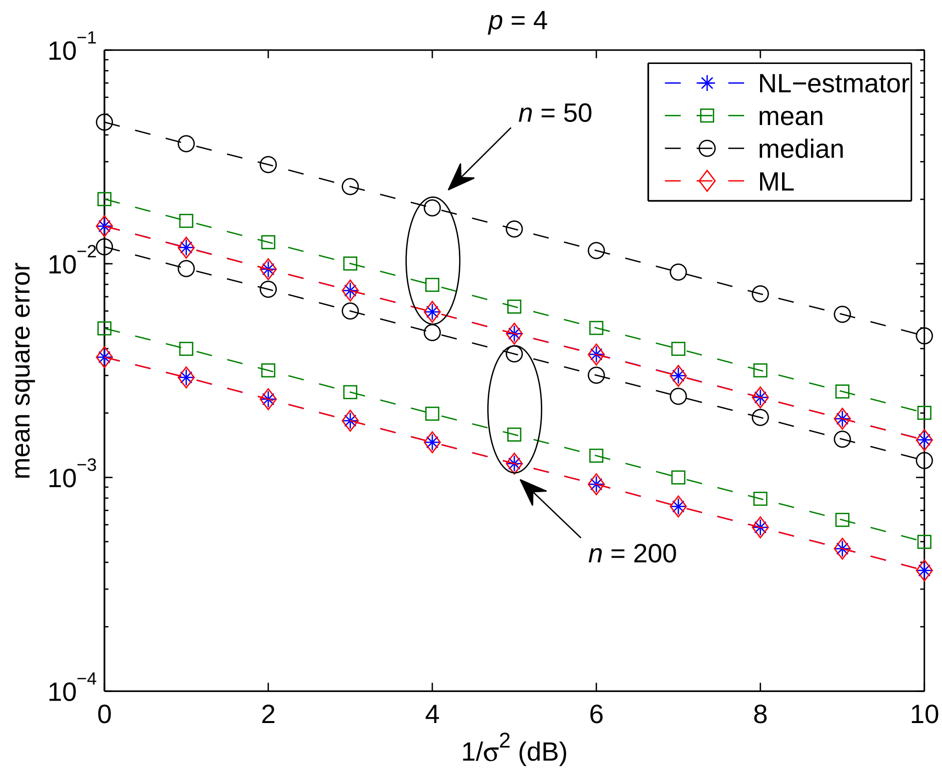

Figure 2.2: The MSEs of the NL-estimaotr, the ML estimator, the mean estimator and the median estimator with $p = 4$.

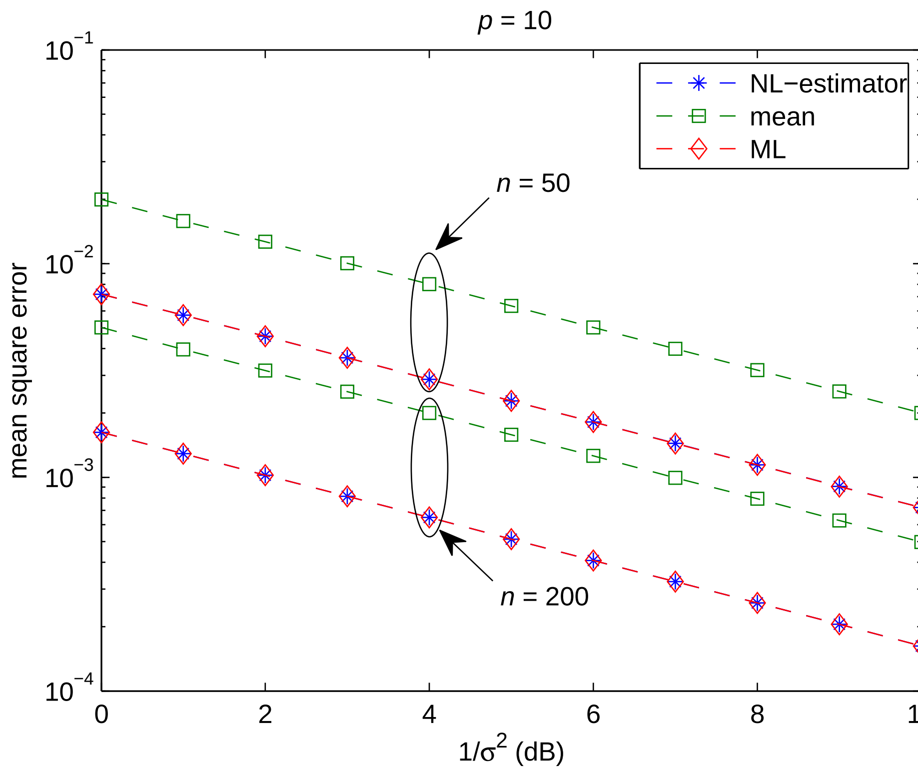

Figure 2.3: The MSEs of the NL-estimator, the ML estimator and the mean estimator with $p = 10$.

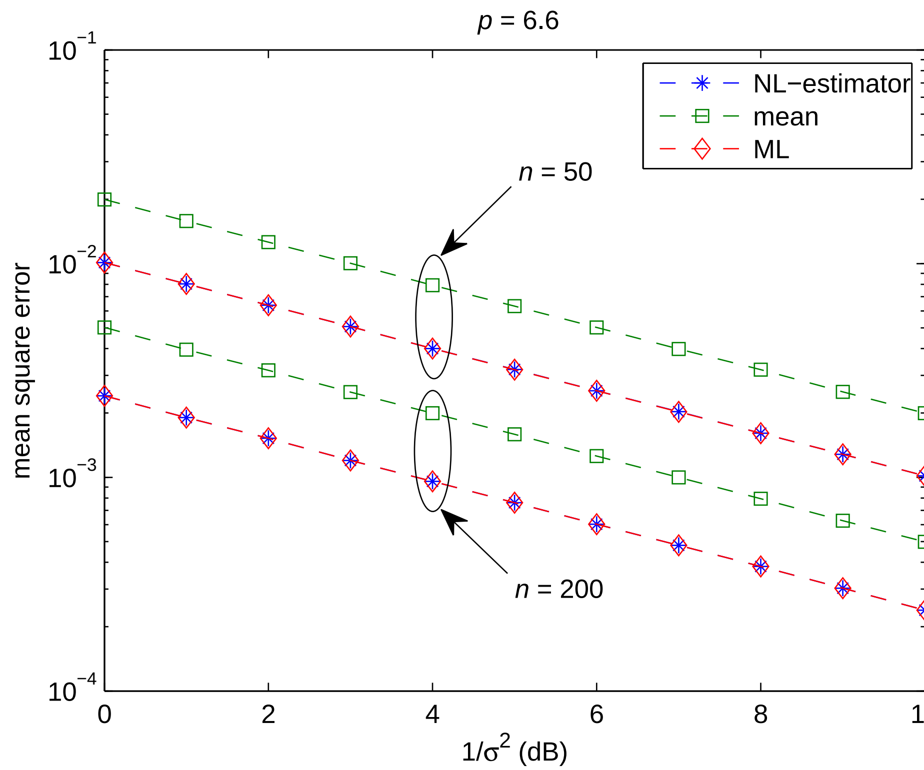

Figure 2.4: The MSEs of the NL-estimator, the ML estimator and the mean estimator with $p = 6.6$.

dB performance gap between the mean estimator and the ML estimator, whereas the loss of the NL-estimator relative to the ML estimator is only 0.002 dB. When $n = 200$, the gap between the mean estimator and the ML estimator increases to about 1.34 dB. However, the gap between the NL-estimator and the ML estimator decreases to about 0.0001 dB and the two curves for the MSE are graphically coincident. The NL-estimator is better than the mean estimator, and for all practical purposes, attains the performance of the ML estimator.

Also shown in Fig. 2.2 is the performance of the median estimator. Recall that the median estimator is optimal for $p = 1$, and the mean estimator is optimal for $p = 2$. We infer that the median estimator will become increasingly inferior to the mean estimator as p increases to larger values from $p = 2$. This behaviour is seen in Fig. 2.2.

Fig. 2.3 compares the MSEs of the NL-estimator, the ML estimator and the mean estimator with $p = 10$. In this simulation, we examine the performance of the NL-estimator in the case of a large shape parameter. For $n = 50$ and $n = 200$, the performance gap between the mean estimator and the ML estimator is about 4.43 dB and 4.88 dB, respectively. The gap between the NL-estimator and the ML estimator is much smaller. It is about 0.006 dB and 0.0003 dB, respectively. In the case of large p, the mean estimator gives decreasing performance compared to $p = 4$, but the NL-estimator still works excellently.

Fig. 2.4 compares the MSEs of the NL-estimator, the ML estimator and the mean estimator with $p = 6.6$. We set $p = 6.6$ to show the performance of the NL-estimator in the case of a non-integer shape parameter. For $n = 50$ and $n = 200$, the performance gap between the mean estimator and the ML estimator is 2.96 dB and 3.18 dB, respectively, whereas the gap between the NL-estimator estimator and the ML estimator is 0.004 dB and 0.0002 dB, respectively. The NL-estimator keeps its advantage over the mean estimator even in the case of non-integer p.

In the rest of this subsection, we will compare the performance of the NL-estimator with the MNS estimator. When the shape parameter is assumed to be known, it means that the shape parameter is estimated exactly. However, it is common that the estimated scale parameter p_e has a small deviation from the true value. If a small deviation results in serious performance degradation, the NL-estimator can not be a robust and applicable estimator.

Fig. 2.5 is the MSEs of the NL-estimator and the MNS estimator when the estimated shape parameter p_e has different deviations from the true value. In Fig. 2.5 the true value is $p = 5.4$. The estimated shape parameter p_e takes values from 4.4 to 6.4. The NL-estimator and the MNS estimator use the estimated value p_e to estimate the location parameter μ. The maximum deviation from the true value $p = 5.4$ is 1 in Fig. 2.5. From the figure, the NL-estimator has an obvious

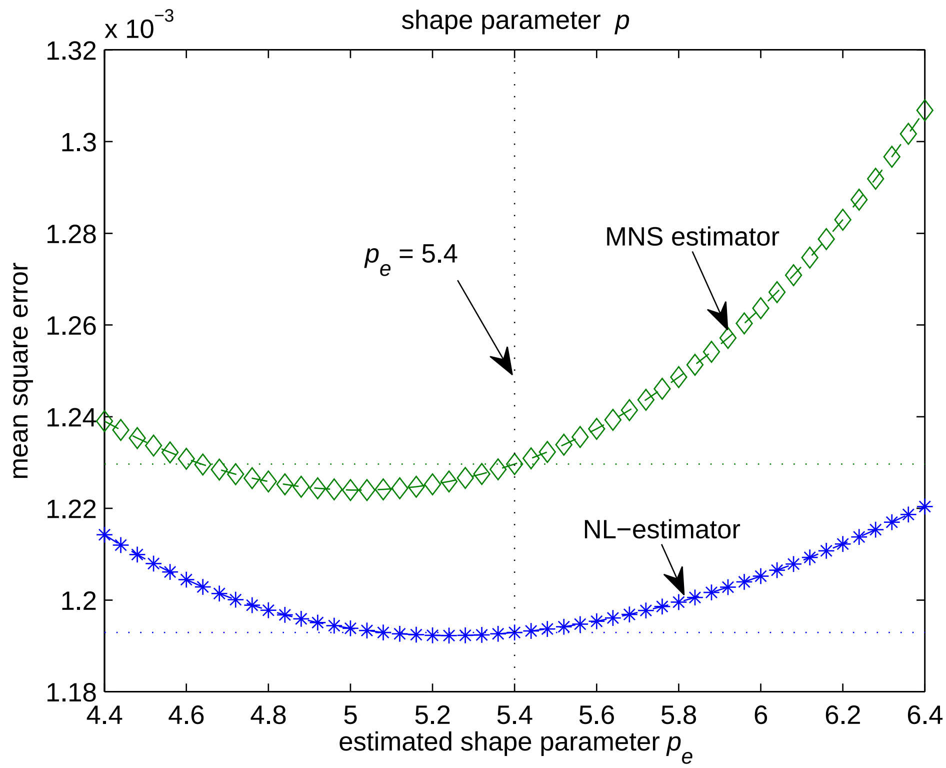

Figure 2.5: The MSEs of the NL-estimator and the MNS estimator when the estimated parameter p_e has different deviations from the true value $p = 5.4$.

advantage over the MNS estimator, no matter whether p_e takes the true value of the shape parameter or not. When $p_e = p = 5.4$, the performance distance between the MNS estimator and the NL-estimator is about 0.1 dB. When p_e takes values on the positive side of 5.4, both estimators has degradating performance and as the deviation increases, the performance degradation is accelerated. The MNS estimator has a faster speed of degradation. When p_e takes values on the negative side of 5.4, an interesting thing is both estimators have sightly better MSE performance at first. Then as the deviation increases, the performance degradation increases and both estimators give worse MSE performance compared with the case of $p_e = p = 5.4$.

Fig. 2.5 shows that the NL-estimator has its advantage over the MNS estimator in terms of MSE performance. Also the NL-estimator is robust to estimate the location parameter when the estimated p_e is not exactly equal to the true value of the shape parameter p. A small deviation from the true value doesn't result in serious performance degradation.

2.4.3 Generalized NL-estimator

In this subsection, we will give a generalized NL-estimator.

A location-scale family is a class of distributions that parametrized by a location parameter μ and the PDF in this class have the form

$$f_\mu(x) = f(x-\mu). \tag{2.47}$$

Let $X_1, X_2, X_3, ..., X_n$ be i.i.d. samples from a symmetric distribution whose PDF $f_\mu(x)$ belongs to a location-scale family. Examples of such distributions include the GGD and the Cauchy distribution. Let $Z_1 \leq Z_2 \leq ... \leq Z_n$ be the order statistics of $X_1, X_2, ..., X_n$.

According to the ML principle, one can have

$$\sum_{i=1}^{n} \frac{\partial}{\partial \mu} \ln f_\mu(x_i|\mu) = 0. \tag{2.48}$$

We want to find approximate solutions of (2.48). The generalized NL-estimator is given as following to solve this problem.

Define two functions $g(\cdot)$ and $h(\cdot)$. The function $g(\cdot)$ is defined as,

$$g(x_i - u) = \frac{\partial}{\partial \mu} \ln f_\mu(x_i|\mu). \tag{2.49}$$

The function $h(\cdot)$ is defined as,

$$h(t) = \frac{\partial}{\partial t} g(t). \tag{2.50}$$

The approximate solution $\hat{\mu}$ of (2.48) is given in this form:

$$\mu_i = \frac{z_i + z_{n-i+1}}{2}, \quad i = 1, 2, ..., n/2 \tag{2.51}$$

$$\hat{\mu} = \sum_{i=1}^{n/2} c_i \mu_i \tag{2.52}$$

where c_i are the coefficients.

The coefficients c_i can be found in this way:

$$d_i = \frac{z_{n-i+1} - z_i}{2} \tag{2.53}$$

$$c_i = \frac{h(d_i)}{\sum_{i=1}^{n/2} h(d_i)}, \quad i = 1, 2, ..., n/2. \tag{2.54}$$

The eqs. (2.51 - 2.54) are the generalized NL-estimator.

Case 1: GGD.

The ML equation for the location parameter μ is

$$\sum_{i=1}^{n} \text{sgn}(x_i - \mu)|x_i - \mu|^{p-1} = 0. \tag{2.55}$$

So the function $g(\cdot)$ (defined in (2.49)) is given as,

$$g(x) = \mathrm{sgn}(x)|x|^{p-1}. \tag{2.56}$$

The function $h(\cdot)$ (defined in (2.50)) is given as,

$$h(t) = \frac{\partial}{\partial t} g(t) = (p-1)t^{p-2}. \tag{2.57}$$

Since

$$d_i = \frac{z_{n-i+1} - z_i}{2} \geq 0 \tag{2.58}$$

the coefficients c_i are given as,

$$c_i = \frac{h(d_i)}{\sum_{i=1}^{n/2} h(d_i)} = \frac{d_i^{p-2}}{\sum_{i=1}^{n/2} d_i^{p-2}}. \tag{2.59}$$

The result is identical with what we have got in Subsection 2.4.1.

Case 2: Cauchy distribution.

The generalized NL-estimator can be applied to the Cauchy distribution as well. Here is the generalized NL-estimator for the Cauchy distribution.

The PDF of the Cauchy distribution with location parameter μ and scale parameter λ is given as,

$$f_\mu(x) = \frac{1}{\pi\lambda\{1 + [(x-\mu)/\lambda]^2\}}. \tag{2.60}$$

According to the ML principle, the ML estimation equation is given as,

$$\sum_{i=1}^{n} \frac{2(x_i - \mu)}{\lambda^2 + (x_i - \mu)^2} = 0. \tag{2.61}$$

From (2.49), $g(\cdot)$ is given as,

$$g(x) = \frac{2x}{\lambda^2 + x^2} \tag{2.62}$$

From (2.50), $h(\cdot)$ is given as,

$$h(t) = \frac{\partial}{\partial t} g(t) = \frac{2(\lambda^2 - t^2)}{(\lambda^2 + t^2)^2}. \tag{2.63}$$

Therefore putting (2.62) and (2.63) into eqs. (2.51 - 2.54), we can get the NL-estimator for the Cauchy distribution.

It is obvious that when $d_i > \lambda$, the corresponding coefficient c_i is negative. It is consistent with the fact that some of weighting factors are negative in [24]. Simulations show that the generalized NL-estimator has much better performance than the highly efficient L-estimator proposed in [24].

2.4.4 Summary

A new unbiased estimator has been proposed for $p \in [2, \infty)$. It was named the NL-estimator. The performances of the NL-estimator, the mean estimator and the ML estimator have been compared. The NL-estimator is superior to the mean estimator, and increasingly so as the shape parameter p is increasingly far from 2. The MSE of the new estimator is almost identical as the MSE of the ML estimator with negligible practical performance loss. The NL-estimator is superior to the MNS estimator as well. When the estimated shape parameter has a small deviation from the true value, the NL-estimator has small performance degradation.

2.5 Approximate ML estimator for $p = 5$

In this section, a closed-form approximate ML estimator for the location parameter of the GGD with $p = 5$ is derived.[5]

2.5.1 Approximate ML estimator for $p = 5$

Let $X_1, X_2, ..., X_n$ be independent and identically distributed (i.i.d.) random samples from a GGD with location parameter μ, shape parameter p and the variance σ^2. Define a vector $\bar{X} = [X_1, X_2, ..., X_n]$. The ML estimation equation was given in (2.4), which is,

$$\sum_{i=1}^{n} \text{sgn}(x_i - \mu)|x_i - \mu|^{p-1} = 0 \tag{2.4}$$

When $p = 5$, the ML estimation equation becomes,

$$\sum_{i=1}^{n} \text{sgn}(x_i - \mu)(x_i - \mu)^4 = 0 \tag{2.64}$$

where sgn denotes the signum function given as [14].

According to the ML principle, the solution of (2.4) is the ML estimator for the location parameter μ. Unfortunately, eq. (2.4) is a transcendental equation due to the signum function and there is no exact closed-form solution. Therefore, approximation is required to eliminate the effect of the signum function to reach a closed-form estimator.

Noting that the PDF of the GGD is symmetric about the location parameter μ, it is intuitive to try the approximation,

$$\mu \approx \text{median}(x_i) \tag{2.65}$$

where the median is defined as the middle order statistic if the sample size n is odd, and the average of the middle two order statistics if the sample size n is even. The order statistics of $\{X_i\}_{i=1}^n$ are defined as $\{Z_i\}_{i=1}^n$, where $Z_1 \leq Z_2 \leq ... \leq Z_n$. Therefore,

$$\text{median}(x_i) = \begin{cases} z_{\frac{n+1}{2}}, & n = 2k+1 \\ \frac{z_{\frac{n}{2}} + z_{\frac{n}{2}+1}}{2}, & n = 2k \end{cases}. \tag{2.66}$$

Using this assumption in the signum function in (2.4), one obtains

$$\sum_{i=1}^{n} \text{sgn}(x_i - \text{median}(x_i))(x_i - \mu)^4 = 0. \tag{2.67}$$

[5] The work in this section has been published in *IEEE Signal Processing Letters* [13].

Expanding (2.67), the new ML estimation equation is given as,

$$\sum_{i=\frac{n}{2}+1}^{n} (z_i - \mu)^4 - \sum_{i=1}^{\frac{n}{2}} (z_i - \mu)^4 = 0 \tag{2.68}$$

if n is even, and

$$\sum_{i=\frac{n+1}{2}+1}^{n} (z_i - \mu)^4 - \sum_{i=1}^{\frac{n-1}{2}} (z_i - \mu)^4 = 0 \tag{2.69}$$

if n is odd.

Note that in (2.69), the sample median $Z_{\frac{n+1}{2}}$ is ignored since $\text{sgn}(0) = 0$. This indicates that when n is odd, the samples can be preprocessed by discarding the sample median and the sample size is always kept even. Therefore, the odd case is not considered in the sequel.

Eq. (2.68) is expanded into its standard polynomial form,

$$\begin{aligned} 4 \cdot \Big(\sum_{i=\frac{n}{2}+1}^{n} z_i - \sum_{j=1}^{\frac{n}{2}} z_j\Big) \cdot \mu^3 - 6 \cdot \Big(\sum_{i=\frac{n}{2}+1}^{n} z_i^2 - \sum_{j=1}^{\frac{n}{2}} z_j^2\Big) \cdot \mu^2 + \\ 4 \cdot \Big(\sum_{i=\frac{n}{2}+1}^{n} z_i^3 - \sum_{j=1}^{\frac{n}{2}} z_j^3\Big) \cdot \mu - \Big(\sum_{i=\frac{n}{2}+1}^{n} z_i^4 - \sum_{j=1}^{\frac{n}{2}} z_j^4\Big) = 0 \end{aligned} \tag{2.70}$$

where the coefficient of μ^4 is zero. Comparing (2.70) with the monic cubic equation, $\mu^3 + a \cdot \mu^2 + b \cdot \mu + c = 0$, the coefficients of each term are respectively,

$$a = \frac{-3 \cdot (\sum_{i=\frac{n}{2}+1}^{n} z_i^2 - \sum_{j=1}^{\frac{n}{2}} z_j^2)}{2 \cdot (\sum_{i=\frac{n}{2}+1}^{n} z_i - \sum_{j=1}^{\frac{n}{2}} z_j)} \tag{2.71}$$

$$b = \frac{(\sum_{i=\frac{n}{2}+1}^{n} z_i^3 - \sum_{j=1}^{\frac{n}{2}} z_j^3)}{(\sum_{i=\frac{n}{2}+1}^{n} z_i - \sum_{j=1}^{\frac{n}{2}} z_j)} \tag{2.72}$$

$$c = \frac{-(\sum_{i=\frac{n}{2}+1}^{n} z_i^4 - \sum_{j=1}^{\frac{n}{2}} z_j^4)}{4 \cdot (\sum_{i=\frac{n}{2}+1}^{n} z_i - \sum_{j=1}^{\frac{n}{2}} z_j)}. \tag{2.73}$$

We will use the cubic formula [20] to find the roots of the cubic equation (2.70).

Five ancillary variables are defined to express the roots of (2.70),

$$t_1 = \frac{(3b - a^2)}{3} \tag{2.74a}$$

$$t_2 = \frac{2a^3 - 9ab + 27c}{27} \tag{2.74b}$$

$$\Delta = -4t_1^3 - 27t_2^2 \tag{2.74c}$$

$$A = \sqrt[3]{-\frac{27}{2}t_2 + \frac{3}{2}\sqrt{-3\Delta}} \tag{2.74d}$$

$$B = \frac{-3t_1}{A} \tag{2.74e}$$

where Δ is the discriminant. For a cubic equation with real coefficients, if $\Delta > 0$, the equation has three distinct real roots; if $\Delta < 0$, the equation has one real root and two complex conjugate roots; if $\Delta = 0$, the equation has a double real root and a simple real root, or a triple real root [19].

The roots of a cubic equation are given by [20, p. 23],

$$r_1 = \frac{1}{3}(A + B - a) \tag{2.75a}$$

$$r_2 = \frac{1}{3}(\rho A + \rho^2 B - a) \tag{2.75b}$$

$$r_3 = \frac{1}{3}(\rho^2 A + \rho B - a) \tag{2.75c}$$

where $\rho = -\frac{1}{2} + \frac{1}{2}\sqrt{-3} = e^{2\pi i/3}$. Note that whatever value the discriminant Δ takes, r_1 is always real. This root is chosen as the approximate ML estimator for the location parameter; that is

$$\mu_{appr} = \frac{1}{3}(A + B - a) \tag{2.76}$$

where A, B and a have been defined above. Simulations in Section 2.5.2 will show that the approximate ML estimator (2.76) is superior to all known closed-form estimators for $p = 5$.

2.5.2 Numerical results and discussion

In this subsection, simulation results are presented to show the performance of the new approximate ML estimator. The approximate ML estimator is compared with the mean estimator, the NL-estimator, the MNS estimator and the numerical ML estimator using Newton's method [22] through the mean square error (MSE) estimated by Monto Carlo simulation. The number of trials used in the Monton Carlo simulation is 2.5×10^7. The Cramér Rao lower bound (CRLB) obtained in Section 2.2 is also plotted in the figures. The signal-to-noise ratio (SNR) is defined as,

$$\text{SNR} = \frac{\mu^2}{\sigma^2}. \tag{2.77}$$

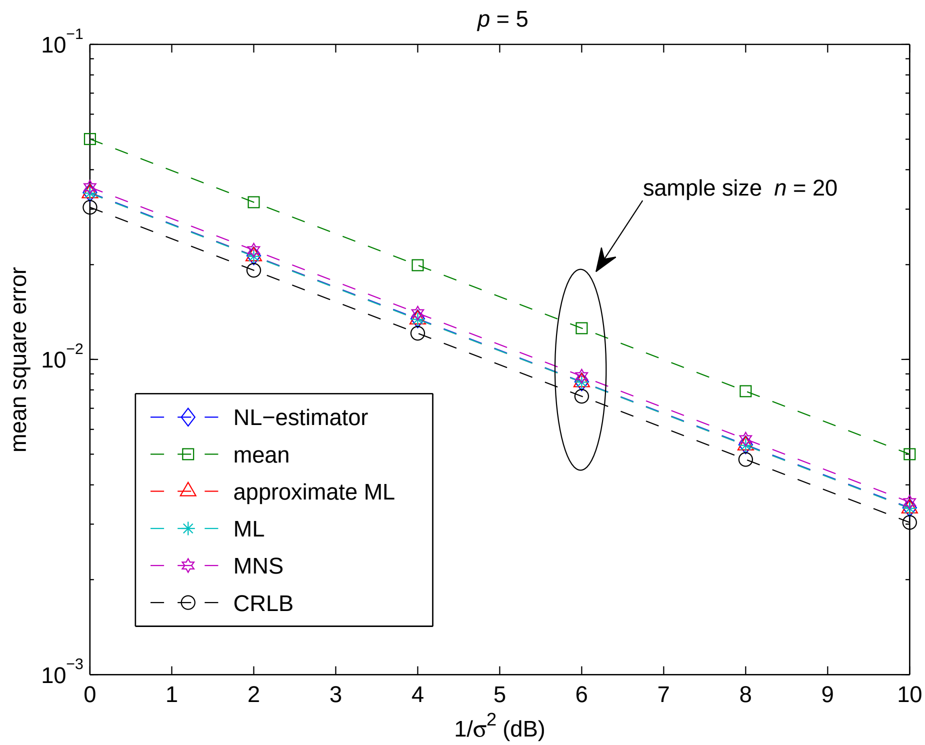

Figure 2.6: The MSEs of the new approximate ML estimator, the NL-estimator, the mean estimator, the numerical ML estimator and the MNS estimator together with the CRLB for $n = 20$.

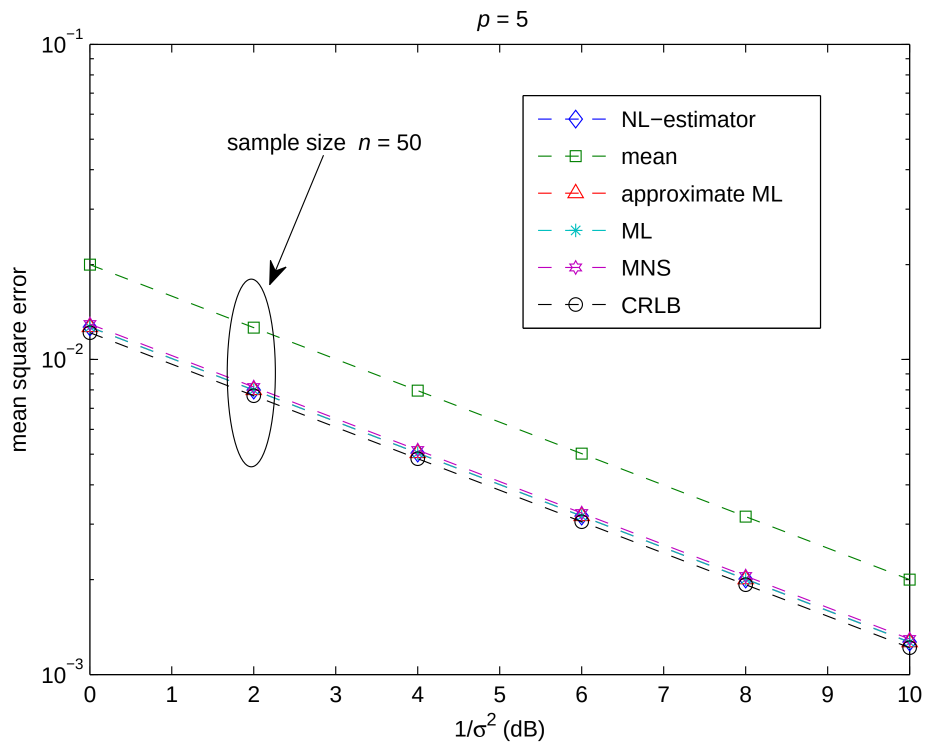

Figure 2.7: The MSEs of the new approximate ML estimator, the NL-estimator, the mean estimator, the numerical ML estimator and the MNS estimator together with the CRLB for $n = 50$.

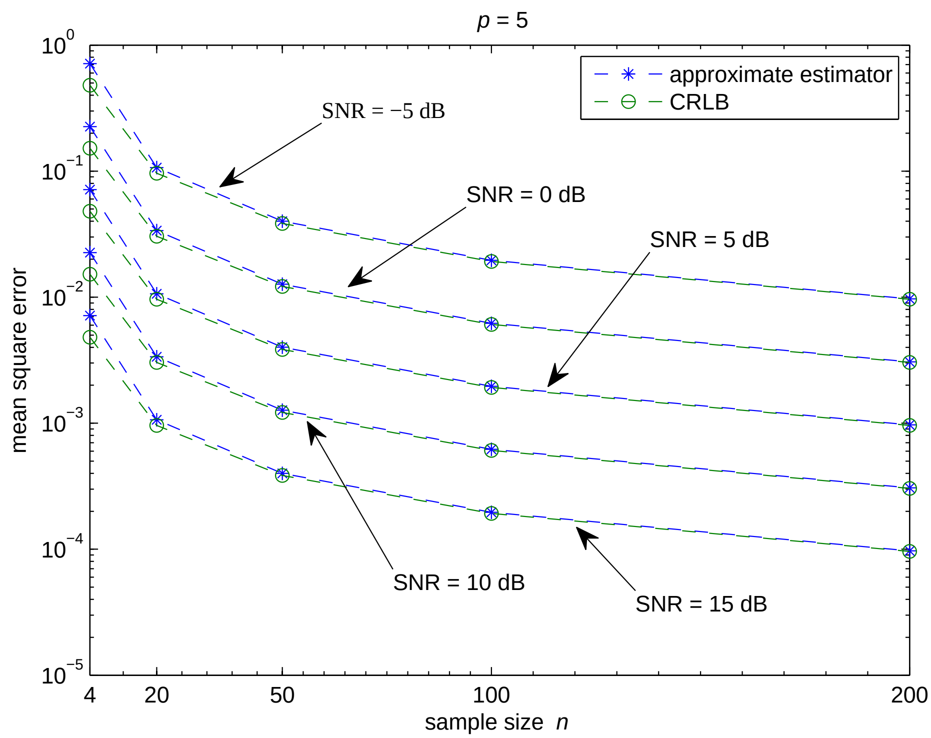

Figure 2.8: The MSEs of the new approximate ML estimator and the CRLB as functions of the number of samples for several values of SNR.

In all the figures, the location parameter μ is fixed at $\mu = 1$.

In making comparisons between the estimators, the following context is important. The mean estimator, the NL-estimator, the new approximate ML estimator and the numerical estimator using Newton's method do not require knowledge of σ^2, while the MNS estimator does. The only estimator which does not require knowledge of σ^2 and performs worse than the MNS estimator, is the mean estimator. All the other estimators considered here perform better than the MNS estimator without requiring knowledge of σ^2. Therefore, compared to other estimators, the MNS estimator has higher complexity and poorer performance except for the mean estimator.

Fig. 2.6 and Fig. 2.7 show the MSEs of the new approximate ML estimator, the NL-estimator, the mean estimator and the MNS estimator. The mean estimator gives the worst performance for both $n = 20$ and $n = 50$. The new approximate ML estimator gives better MSE performance compared to the NL estimator and the MNS estimator. For $n = 20$ and $n = 50$, the approximate estimator has an advantage of 0.014 dB and 0.0025 dB over the NL-estimator and has an advantage of 0.19 dB and 0.1 dB over the MNS estimator.

Fig. 2.6 and Fig. 2.7 also show the MSE of the numerical ML estimator and the CRLB. The numerical ML estimator is calculated using Newton's method. For $n = 20$ and $n = 50$, its MSE gains relative to the new approximate estimator are only 7×10^{-4} dB and 5×10^{-5} dB, respectively. The gap between the numerical ML estimator and the CRLB is 0.45 dB for $n = 20$ and decreases to 0.17 dB when the number of samples increases to $n = 50$.

Fig. 2.8 gives the MSEs of the new approximate estimator and the CRLB when the sample size n increases from 4 to 200 for several values of SNR. One can see that the SNR gap between the MSE of the new estimator and CRLB is very small, and decreases as the number of samples increases. The simulation results indicate that the MSE of the new estimator attains the CRLB, for all practical purposes, for $n \geq 20$. For all values of SNR between -5 dB and 15 dB, the greatest MSE of the new estimator is only 1.5 times the CRLB. For $n = 4$, n= 20, $n = 50$, $n = 100$ and $n = 200$, the corresponding gaps are 1.72 dB, 0.45 dB, 0.17 dB, 0.088 dB and 0.045 dB, respectively.

2.5.3 Summary

A novel closed-form approximate ML estimator for the location parameter of the GGD when the shape parameter $p = 5$ was derived in this section. The approximate ML estimator gives the best MSE performance compared to previous estimators while having comparable complexity.

Chapter 3

Asymptotic performance analysis of an optimal detector in generalized Gaussian noise

3.1 Optimal detector

The baseband system model is shown in Fig. 3.1 [25]. The binary symbol d takes values $+1$ or -1 with equal probabilities and modulates an arbitrary time-limited pulse shape $s(t)$. The signal $d \cdot s(t)$ is transmitted over a distortionless channel with additive generalized Gaussian noise and then the signal $x(t) = d \cdot s(t) + n(t)$ is received. Before the received signal $x(t)$ is processed by the detector, $x(t)$ is filtered by an ideal low-pass filter to remove the out-of-band noise.

The pulse shape $s(t)$ is assumed to be

$$s(t) = \begin{cases} > 0, \text{for all } t \in [0, T] \\ 0, \quad \text{otherwise} \end{cases} . \tag{3.1}$$

There is no loss of generality in assuming (3.1) if $n(t)$ is white or strictly white noise since if $s(t) < 0$ in some regions of $[0, T]$, $x(t)$ can be preprocessed by multiplying $s(t)$ by -1 in these regions. Also the pulse shape $s(t)$ is assumed to be band-limited to B Hz. Strictly speaking, band-limited signals cannot be time-limited. However in practice, the energy of a signal is considered to be within a frequency range of $B \gg 1/T$ [25]. The waveform of $s(t)$ is known at the receiver side. The two-sided power spectral density of generalized Gaussian noise is assumed to be $N_0/2$.

In the discrete-time case, the detector samples the signal $r(t)$ at a rate of $2B$ per second, giving $M = 2BT$ noisy samples when a symbol d is transmitted; they are

$$r_i = d \cdot s_i + n_i, i = 1, 2, \ldots, M. \tag{3.2}$$

The M samples at this sampling rate can be considered to be uncorrelated if the noise is white and independent if the noise is strictly white [26, p. 385]. Since

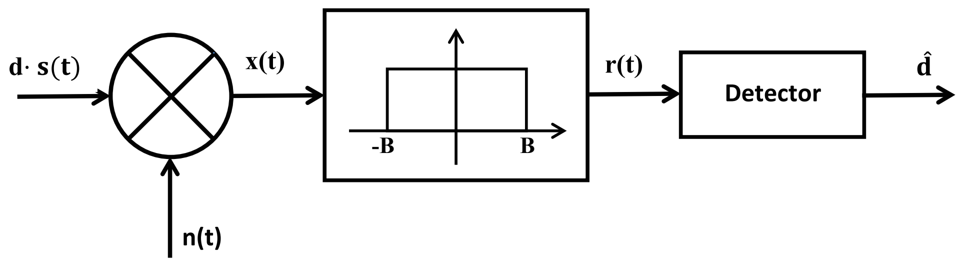

Figure 3.1: Block diagram of the system model.

$s(t) > 0$ for $t \in [0, T]$, s_i are positive. The n_i in (3.2) are generalized Gaussian noise samples with zero mean, and variance $\sigma^2 = N_0 B$. The PDF of the generalized Gaussian samples is given in Chapter 1,

$$f(x) = \frac{1}{2\Gamma(1 + 1/p)\alpha} \exp\left\{-\left(\frac{|x - \mu|}{\alpha}\right)^p\right\} \tag{1.1a}$$

$$\alpha = \left[\frac{\sigma^2 \Gamma(1/p)}{\Gamma(3/p)}\right]^{\frac{1}{2}} \tag{1.1b}$$

where p is the shape parameter. When $p = 1$, generalized Gaussian noise becomes Laplace noise. When $p = 2$, generalized Gaussian noise becomes Gaussian noise.

The detection problem can be modeled as the following hypothesis test,

$$H_0 : r_i = -s_i + n_i \tag{3.4}$$

$$H_1 : r_i = s_i + n_i \tag{3.5}$$

$$i = 1, \ldots, M. \tag{3.6}$$

Define $\bar{r} = (r_1, r_2, \ldots, r_M)$. The log-likelihood ratio is

$$\begin{aligned} l &= \ln \frac{f(\bar{r}|H_1)}{f(\bar{r}|H_0)} \\ &= \sum_{i=1}^{M} \left[-\frac{|r_i - s_i|^p}{\alpha^p} + \frac{|r_i + s_i|^p}{\alpha^p}\right] && (3.7) \\ &= \sum_{i=1}^{M} \frac{1}{\alpha^p} y_i && (3.8) \end{aligned}$$

where the variables y_i are defined as,

$$y_i = -|r_i - s_i|^p + |r_i + s_i|^p. \tag{3.9}$$

The log-likelihood ratio test (LRT) is

$$l = \sum_{i=1}^{M} \frac{1}{\alpha^p} y_i \underset{H_0}{\overset{H_1}{\gtrless}} \ln \frac{\Pr(d = -1)}{\Pr(d = +1)} = \tau \tag{3.10}$$

where τ is the threshold. Since we have assumed the binary symbol d takes values $+1$ or -1 with equal probabilities,

$$\Pr(d=-1)=\Pr(d=+1)=\frac{1}{2} \tag{3.11}$$

the threshold τ is equal to 0. The optimal discrete-time detector (3.10) decides $d=+1$ if $l>0$ and decides $d=-1$ if $l<0$. The detector equally likely decides $d=+1$ or $d=-1$ when $l=0$.

In the special case of the Laplace distribution, namely $p=1$, by defining $g_i(t)$ as,

$$g_i(t)=\frac{1}{\alpha}(-|t-s_i|+|t+s_i|) \tag{3.12}$$

$$=\begin{cases}\frac{2s_i}{\alpha}, & \text{if } t\geq s_i\\ \frac{2t}{\alpha}, & \text{if} -s_i<t<s_i\\ -\frac{2s_i}{\alpha}, & \text{if } t\leq -s_i\end{cases} \tag{3.13}$$

where $s_i>0$, the LRT is given in [27],

$$l=\sum_{i=1}^{M}\frac{1}{\alpha}\left(-|r_i-s_i|+|r_i+s_i|\right) \tag{3.14}$$

$$=\sum_{i=1}^{M}g_i(r_i)\underset{H_0}{\overset{H_1}{\gtrless}}0. \tag{3.15}$$

In the special case of the Gaussian distribution, namely p =2, the LRT is,

$$l=\sum_{i=1}^{M}\frac{4r_is_i}{\alpha^2}\underset{H_0}{\overset{H_1}{\gtrless}}0. \tag{3.16}$$

The simplified LRT is,

$$l=\sum_{i=1}^{M}r_is_i\underset{H_0}{\overset{H_1}{\gtrless}}0. \tag{3.17}$$

Eqs. (3.17) and (3.14) show that the matched-filter detector is optimal for detection in additive white Gaussian noise and suboptimal in additive white Laplace noise.

In the rest of this chapter, the asymptotic performance of the optimal detection structure will be analyzed in the presence of bandlimited white generalized Gaussian noise by using the Gaussian approximation method.

3.2 Gaussian approximation

In non-Gaussian detection, performance analysis for the detector is frequently a complicated mathematical problem. In many cases, if the sample size is sufficiently large, a central limit theorem (CLT) [26, p. 278] is used to approximate the distribution function of the test statistic [28]. The invocation of a CLT is justified by positing that the samples are independent. More generally, one could use a less restrictive posit that the samples may be independent or dependent[1], but satisfy a CLT. Then, when the sample size M is sufficiently large, the test statistic l of the optimal detector approaches a Gaussian distribution with mean μ and variance σ^2. Provided that the mean μ and the variance σ^2 for $d = +1$ are known, the Gaussian approximation for the bit error rate (BER) of the optimal detector in generalized Gaussian noise is given as,

$$\mathrm{P}_e = Q(\frac{\mu - \tau}{\sigma}) = Q(\frac{\mu}{\sigma}) \tag{3.18}$$

where $Q(\cdot)$ denotes the Q-function which is defined in [31] as,

$$Q(x) = \frac{1}{\sqrt{2\pi}} \int_x^\infty \exp\left(-\frac{z^2}{2}\right) \mathrm{d}z. \tag{3.19}$$

We will only consider independent samples in the sequel, but point out that the dependent sample case can also be treated similarly with more cumbersome and lengthy mathematics.

3.3 Asymptotic performance analysis

It is a mathematically cumbersome problem to derive a closed-form expression for μ and σ^2 for arbitrary $p > 0$. In this section, the shape parameter p takes integer values and the Gaussian approximation for the BER of the optimal detector in generalized Gaussian noise is derived for the case where the sample size M approaches infinity.

When $d = +1$ is transmitted and $M \to \infty$, the mean of the test statistic l is determined as,

$$\mu = E(l) = E\left(\lim_{M\to\infty} \sum_{i=1}^{M} \frac{1}{\alpha^p} y_i\right)$$

$$= \lim_{M\to\infty} \sum_{i=1}^{M} E(\frac{1}{\alpha^p} y_i) \tag{3.20}$$

where $y_i = -|r_i - s_i|^p + |r_i + s_i|^p$, and r_i are i.i.d. generalized Gaussian random variables with mean $\mu_r = s_i$, variance σ_r^2 and shape parameter p. Similarly, the

[1]Note that just as CLTs exist for independent samples, CLTs also exist for dependent samples. In the case of dependent samples, different requirements on the correlation or dependency between the samples are needed. However, all the conditions reflect the basic intuition that one expects a CLT to hold for dependent random samples, if the samples behave more like independent samples the further the samples are separated [29], [30].

variance of the test statistic l is given by,

$$\sigma^2 = Var(l) = \lim_{M\to\infty} \sum_{i=1}^{M} Var(\frac{1}{\alpha^p} y_i)$$

$$= \lim_{M\to\infty} \sum_{i=1}^{M} E\left[(\frac{1}{\alpha^p} y_i)^2\right] - \left[E(\frac{1}{\alpha^p} y_i)\right]^2. \tag{3.21}$$

Case 1: p is even.

When p is even, $\frac{1}{\alpha^p} y_i$ and $(\frac{1}{\alpha^p} y_i)^2$ can be rearranged as,

$$\frac{1}{\alpha^p} y_i = \sum_{j=0}^{p-1} \binom{p}{j} \left(\frac{r_i - s_i}{\alpha}\right)^j \left(\frac{2 \cdot s_i}{\alpha}\right)^{p-j} \tag{3.22}$$

$$(\frac{1}{\alpha^p} y_i)^2 = \sum_{m=0}^{p-1} \sum_{n=0}^{p-1} \binom{p}{m} \binom{p}{n} \left(\frac{r_i - s_i}{\alpha}\right)^{m+n} \left(\frac{2 \cdot s_i}{\alpha}\right)^{2p-m-n} \tag{3.23}$$

where $\binom{p}{j}$ denotes the binomial coefficient. By using the kth moment of the standardized generalized Gaussian variable available in Section 1.2, one can obtain the expectations of $\frac{1}{\alpha^p} y_i$ and $(\frac{1}{\alpha^p} y_i)^2$.

The expectation of $\frac{1}{\alpha^p} y_i$ is given as,

$$E\left(\frac{1}{\alpha^p} y_i\right) = \sum_{j=0, j\ even}^{p-1} \frac{\Gamma(\frac{j+1}{p})}{\Gamma(1/p)} \binom{p}{j} (\frac{2s_i}{\alpha})^{p-j} \tag{3.24}$$

where $\binom{p}{j}$ denotes the binomial coefficient. The expectation of $(\frac{1}{\alpha^p} y_i)^2$ is given as,

$$E\left[(\frac{1}{\alpha^p} y_i)^2\right] = \sum_{m=0}^{p-1} \sum_{\substack{n=0 \\ m+n \text{ even}}}^{p-1} \frac{\Gamma(\frac{m+n+1}{p})}{\Gamma(1/p)} \binom{p}{m} \binom{p}{n} (\frac{2s_i}{\alpha})^{2p-m-n}. \tag{3.25}$$

Eqs. (3.24) and (3.25) show that the expectation and the variance of $\frac{1}{\alpha^p} y_i$ are polynomials of the form,

$$c_1 \frac{s_i^2}{\alpha^2} + c_2 \frac{s_i^4}{\alpha^4} + c_3 \frac{s_i^6}{\alpha^6} + \ldots. \tag{3.26}$$

Note that when $M \to \infty$, since

$$\sigma^2 = N_0 B = N_0 \cdot \frac{M}{2T} \tag{3.27}$$

one can obtain for an integer $n > 2$,

$$\lim_{M\to\infty} \sum_{i=1}^{M} \frac{s_i^n}{\alpha^n} = \lim_{M\to\infty} \sum_{i=1}^{M} \left(\frac{T}{M}\right)^{\frac{n}{2}-1} \left(\frac{2\Gamma(3/p)}{N_0 \Gamma(1/p)}\right)^{\frac{n}{2}} \cdot \frac{T}{M} s_i^n$$

$$= \lim_{M\to\infty} \sum_{i=1}^{M} \left(\frac{T}{M}\right)^{\frac{n}{2}-1} \left(\frac{2\Gamma(3/p)}{N_0 \Gamma(1/p)}\right)^{\frac{n}{2}} \cdot \int_0^T s(t)^n \mathrm{d}t \to 0. \tag{3.28}$$

Using (3.26) and (3.28), the mean and the variance of the test statistic l from (3.20) and (3.21) can be rearranged into,

$$\mu \approx \lim_{M\to\infty} \sum_{i=1}^{M} c_\mu \frac{s_i^2}{\alpha^2}$$

$$= \lim_{M\to\infty} \sum_{i=1}^{M} \frac{\Gamma(1-1/p)}{\Gamma(1/p)} \cdot \frac{p(p-1)}{2} \cdot \left(\frac{2s_i}{\alpha}\right)^2$$

$$= \lim_{M\to\infty} \sum_{i=1}^{M} \frac{\Gamma(2-1/p)}{\Gamma(1/p)} \cdot \frac{p^2}{2} \cdot \frac{4s_i^2}{(\frac{M}{2T}) \cdot N_0 \cdot \frac{\Gamma(1/p)}{\Gamma(3/p)}}$$

$$= \frac{\Gamma(2-1/p)\Gamma(3/p)}{\Gamma(1/p)^2} \cdot p^2 \cdot \frac{4E_s}{N_0} \tag{3.29}$$

$$\sigma^2 \approx \lim_{M\to\infty} \sum_{i=1}^{M} c_\sigma \frac{s_i^2}{\alpha^2}$$

$$= \lim_{M\to\infty} \sum_{i=1}^{M} \frac{\Gamma(2-1/p)}{\Gamma(1/p)} \binom{p}{p-1} \binom{p}{p-1} \left(\frac{2s_i}{\alpha}\right)^2$$

$$= \frac{\Gamma(2-1/p)\Gamma(3/p)}{\Gamma(1/p)^2} \cdot p^2 \cdot \frac{8E_s}{N_0} \tag{3.30}$$

where $E_s = \int_0^T |s(t)|^2 \mathrm{d}t$.

Case 2: p is odd.

The expectation of $\frac{1}{\alpha^p} y_i$ is given in (3.31) and the expectation of $(\frac{1}{\alpha^p} y_i)^2$ is given in (3.32),

$$E(\frac{1}{\alpha^p} y_i) = \sum_{j=0}^{p-1} \frac{\binom{p}{j}}{2\Gamma(1/p)} (\frac{2s_i}{\alpha})^{p-j} \left\{ [1+(-1)^j]\Gamma(\frac{j+1}{p}) - 2(-1)^j \Gamma\left[\frac{j+1}{p}, (\frac{2s_i}{\alpha})^p\right] \right\}$$
$$- \frac{\Gamma(\frac{p+1}{p}) - \Gamma\left[\frac{p+1}{p}, (\frac{2s_i}{\alpha})^p\right]}{\Gamma(1/p)} \tag{3.31}$$

$$E\left[(\frac{1}{\alpha^p} y_i)^2\right] = \sum_{j=0}^{2p-1} \binom{2p}{j} \frac{1+(-1)^j}{2\Gamma(1/p)} \Gamma(\frac{j+1}{p})(\frac{2s_i}{\alpha})^{2p-j} + 2\frac{\Gamma(\frac{2p+1}{p})}{\Gamma(1/p)}$$
$$+ \sum_{j=0}^{p} \binom{p}{j} \frac{(-1)^{p+j}}{\Gamma(1/p)} (\frac{2s_i}{\alpha})^{p-j} \left\{ [1-(-1)^{p+j}] \cdot \Gamma(\frac{p+j+1}{p}) - 2\Gamma\left[\frac{p+j+1}{p}, (\frac{2s_i}{\alpha})^p\right] \right\} \tag{3.32}$$

where $\Gamma(\cdot,\cdot)$ denotes the incomplete gamma function, which is defined in [20] as,

$$\Gamma(a,x) = \int_x^{\infty} t^{a-1}\exp(-t)\mathrm{d}t. \tag{3.33}$$

The derivation of (3.31) and (3.32) are given as following.

Let $f(\cdot)$ be the PDF of the GGD. One can get the following three integrals in Appendix A.1,

$$\int_{-\infty}^{-s_i}\left(\frac{x-s_i}{\alpha}\right)^k f(x)\mathrm{d}x = \frac{(-1)^k}{2\Gamma(1/p)}\Gamma\left[\left(\frac{k+1}{p}\right),\left(\frac{2s_i}{\alpha}\right)^p\right] \tag{3.34}$$

$$\int_{-s_i}^{s_i}\left(\frac{x-s_i}{\alpha}\right)^k f(x)\mathrm{d}x = \frac{(-1)^k}{2\Gamma(1/p)}\left\{\Gamma(\frac{k+1}{p}) - \Gamma\left[\left(\frac{k+1}{p}\right),\left(\frac{2s_i}{\alpha}\right)^p\right]\right\} \tag{3.35}$$

$$\int_{s_i}^{\infty}\left(\frac{x-s_i}{\alpha}\right)^k f(x)\mathrm{d}x = \frac{1}{2\Gamma(1/p)}\Gamma\left(\frac{k+1}{p}\right) \tag{3.36}$$

where k is an integer.

When p is odd, the expectation of $\frac{1}{\alpha^p}y_i$ is

$$E(\frac{1}{\alpha^p}y_i) = \int_{-\infty}^{-s_i}\frac{y_i}{\alpha^p}f\mathrm{d}r_i + \int_{-s_i}^{s_i}\frac{y_i}{\alpha^p}f\mathrm{d}r_i + \int_{s_i}^{\infty}\frac{y_i}{\alpha^p}f\mathrm{d}r_i. \tag{3.37}$$

Using the integrals (3.34), (3.35) and (3.36), one can obtain (3.31) from (3.37). Then, $(\frac{1}{\alpha^p}y_i)^2$ can be written as,

$$(\frac{1}{\alpha^p}y_i)^2 = 2\left(\frac{r_i-s_i}{\alpha}\right)^{2p} + \sum_{j=0}^{2p-1}\binom{2p}{j}\left(\frac{r_i-s_i}{\alpha}\right)^{2p-j} - \frac{|r_i^2-s_i^2|^p}{\alpha^{2p}}. \tag{3.38}$$

Using the kth moment of the standardized generalized Gaussian variable, one can get

$$E\left[2\left(\frac{r_i-s_i}{\alpha}\right)^{2p} + \sum_{j=0}^{2p-1}\binom{2p}{j}\left(\frac{r_i-s_i}{\alpha}\right)^{2p-j}\right]$$

$$= \sum_{j=0}^{2p-1}\binom{2p}{j}\frac{1+(-1)^j}{2\Gamma(1/p)}\Gamma(\frac{j+1}{p})(\frac{2s_i}{\alpha})^{2p-j} + 2\frac{\Gamma(\frac{2p+1}{p})}{\Gamma(1/p)}. \tag{3.39}$$

Using the integrals (3.34), (3.35) and (3.36), one can get,

$$E\left(-\frac{|r_i^2-s_i^2|^p}{\alpha^{2p}}\right)$$

$$= \sum_{j=0}^{p}\binom{p}{j}\frac{(-1)^{p+j}}{\Gamma(1/p)}(\frac{2s_i}{\alpha})^{p-j}\left\{[1-(-1)^{p+j}]\cdot\Gamma(\frac{p+j+1}{p}) - 2\Gamma\left[\frac{p+j+1}{p},(\frac{2s_i}{\alpha})^p\right]\right\}. \tag{3.40}$$

Eq. (3.32) is the summation of (3.39) and (3.40).

The Taylor series expansions of (3.31) and (3.32) around the point $\frac{s_i}{\alpha} = 0$ are given as,

$$E(\frac{1}{\alpha^p}y_i) = c_\mu(\frac{s_i}{\alpha})^2 + o\left((\frac{s_i}{\alpha})^2\right) \tag{3.41}$$

$$E\left[(\frac{1}{\alpha^p}y_i)^2\right] = c_\sigma(\frac{s_i}{\alpha})^2 + o\left((\frac{s_i}{\alpha})^2\right) \tag{3.42}$$

where $o(\cdot)$ is little o notation [32] and where c_μ and c_σ are the corresponding coefficients. The constants c_μ and c_σ are given as,

$$c_\mu = 2p^2 \cdot \frac{\Gamma(2-1/p)}{\Gamma(1/p)} \tag{3.43}$$

$$c_\sigma = 4p^2 \cdot \frac{\Gamma(2-1/p)}{\Gamma(1/p)}. \tag{3.44}$$

Therefore, the mean and the variance of the test statistic l with odd p have the same structure as the mean and the variance for the even case; they are,

$$\mu \approx \lim_{M\to\infty} \sum_{i=1}^{M} c_\mu \frac{s_i^2}{\alpha^2} = \frac{\Gamma(2-1/p)\Gamma(3/p)}{\Gamma(1/p)^2} \cdot p^2 \cdot \frac{4E_s}{N_0} \tag{3.45}$$

$$\sigma^2 \approx \lim_{M\to\infty} \sum_{i=1}^{M} c_\sigma \frac{s_i^2}{\alpha^2} = \frac{\Gamma(2-1/p)\Gamma(3/p)}{\Gamma(1/p)^2} \cdot p^2 \cdot \frac{8E_s}{N_0}. \tag{3.46}$$

Combining case 1 and case 2 together, one can obtain that when p is an integer, the asymptotic BER of the optimal detector in generalized Gaussian noise is given as,

$$P_{e,\mathrm{GA}} = Q(\frac{\mu}{\sigma}) = Q\left(\sqrt{\frac{\Gamma(2-1/p)\Gamma(3/p)}{\Gamma(1/p)^2} \cdot p^2 \cdot \frac{2E_s}{N_0}}\right). \tag{3.47}$$

When the shape parameter p increases to a certain value, the test statistic l may not satisfy the CLT. It is a complicate mathematical problem. In underwater acoustic communications, the shape parameter of generalized Gaussian noise typically ranges from 1.4 to 6 [33]. Simulations in next section will test the asymptotic BER (3.47) for $p \in [1, 6]$. The range of p in (3.47) can be investigated in the future.

3.4 Numerical results and discussion

In this subsection, simulations are performed to verify the theoretical analysis. The example pulse shape $s(t)$ is a half-sine pulse and the time duration T is π seconds.

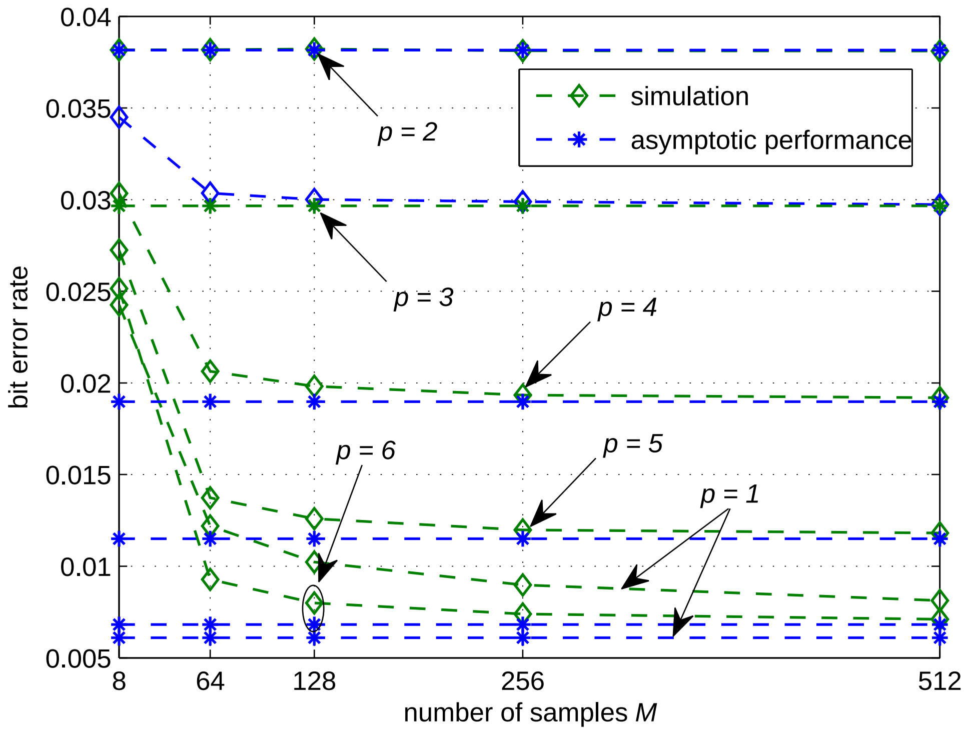

Figure 3.2: The detector performance when p is an integer.

The pulse samples s_i are given as,

$$s_i = \sin(\frac{\pi}{M} i), \quad i = 1, \ldots, M. \tag{3.48}$$

The power spectral density is $\frac{N_0}{2} = \frac{1}{2}$. Fig. 3.2 shows the behavior of the optimal detector when p is an integer, $p = 1$, 2, 3, 4, 5 and 6. When p is 2, 3, 4, 5 or 6, the detector attains the asymptotic BER for about 128 samples or less. Fig. 3.3 shows that (3.47) can also be applied to the non-integer p case. So one can broaden the scope of (3.47) from integer cases to non-integer cases. Once again, the asymptotic BER is achieved for about 128 samples or fewer. Both Fig. 3.2 and Fig. 3.3 show that when the shape parameter p is near 1, the detector slowly converges to its performance asymptote.

3.5 Summary

In this chapter, an optimal detector for generalized Gaussian noise was derived. A central limit theorem was invoked when the number of samples is sufficiently large, and then based on the Gaussian approximation method, a closed-form expression for the asymptotic performance of the detector was derived when the shape param-

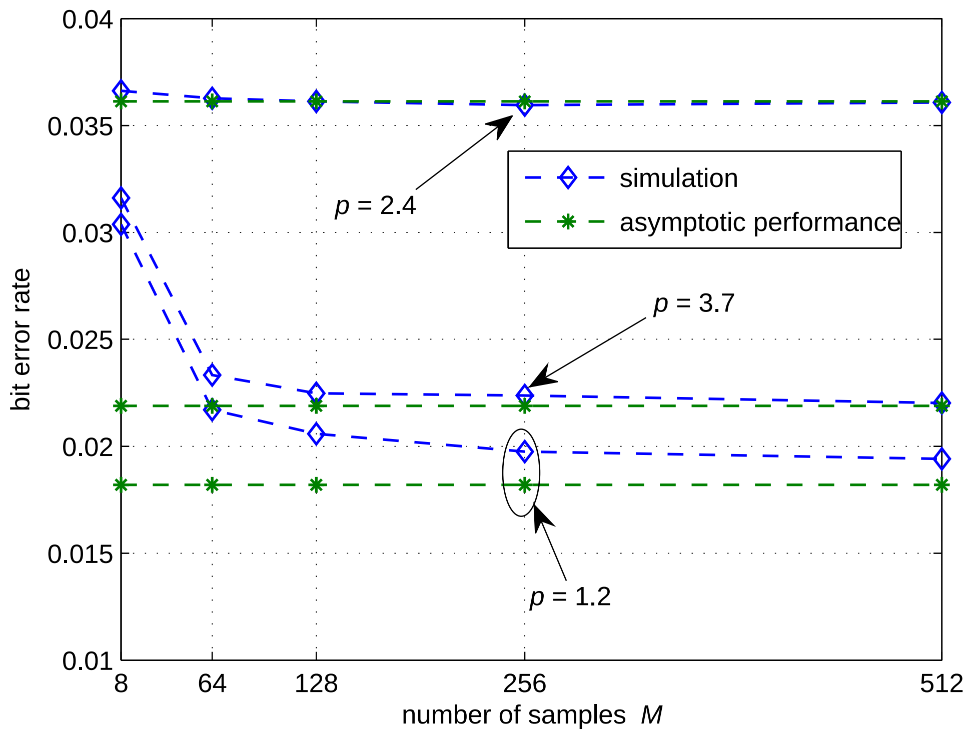

Figure 3.3: The detector performance when p is a non-integer.

eter p is an integer. Numerical results validated the expression for the asymptotic performance for $p \in [1, 6]$.

Chapter 4

Conclusions

4.1 Conclusions

In this thesis, estimators for the location parameter of the GGD and an optimal detector for generalized Gaussian noise were investigated. Highlights of the research results can be summarized as:

- Maximum likelihood estimation of the GGD was discussed. A closed-form expression for the Cramér Rao lower bound was derived.
- There were only three values of p for which the exact ML estimator is known in an explicit form. The proposed exact ML estimator for $p = 4$ increases the number up to 4.
- The unbiased NL-estimator could be applied for $p \in [2, \infty)$. The MSE of the NL-estimator is superior to the mean estimator and the MNS estimator. In terms of robustness, the NL-estimator is better than the MNS estimator as well. The generalized NL-estimator was given.
- The approximate ML estimator for $p = 5$ is the best closed-form estimator known for $p = 5$.
- An optimal detector for generalized Gaussian distributed noise was derived. The asymptotic BER performance of the detector was analysed theoretically by using the Gaussian approximation method. A closed-form expression for the asymptotic BER performance was obtained for $p \in [1, 6]$ and validated by numerical examples.

4.2 Future research directions

The research work in this thesis provides some new results of estimation and detection of the GGD. The methodology and techniques used in this thesis also give insights into possible future research directions in this area. Based on results from this thesis, some possible future research directions are recommended below.

- In Section 2.2, the closed-form expression for the CRLB was obtained. However, the CRLB cannot hold for the uniform distribution. One potential research direction is to investigate the domain of p in the CRLB expression (2.17).
- In Section 2.4, the generalized NL-estimator was introduced, and simulations showed that it could be applied to both the GGD and the Cauchy distribution. It will be an interesting topic to investigate other distributions on which the generalized NL-estimator can be used.
- In applications, the sample size is not possible to be infinite. In Chapter 3, only the asymptotic BER performance of the optimal detector was investigated. One can continue to study the BER performance of the detector with a given sample size.

Bibliography

[1] P. A. Nielsen and J. Thomas, “Signal detection in Arctic under-ice noise”, *Proc. 25th Annu. Alerton Conf. Commun., Cont., Comput.*, pp. 172-177, Oct, 1987.

[2] X. Yang, M. Li and X. Zhao, “Optimum detectors of line spectrum signals in generalized Gaussian noise”, *Proc. 2011 3rd Int. Conf. ICMTMA*, pp. 819-822, Jan. 2011.

[3] N. C. Beaulieu, H. Shao and J. Fiorina, “P-order metric UWB receiver structures with superior performance”, *IEEE Trans. Commun.*, vol. 56, no. 10, pp. 1666-1675, Oct. 2008.

[4] J. K. Su and R. M. Mersereau, “Coding using Gaussian mixture and generalized Gaussian models”, *Proc. IEEE Int. Conf. Image Process.*, pp. 217-220, Sep. 1996.

[5] J. Chen, J. N. Yanez, and A. Achim, “Video super-resolution using generalized Gaussian Markov random fields”, *IEEE Signal Process. Lett.*, vol. 19, pp. 63-66, Feb. 2012.

[6] X. Zou, P. Jancovic, J. Liu, and M. Kokuer, “Speech signal enhancement based on MAP algorithm in the ICA space”, *IEEE Trans. Signal Process.*, vol. 56, May 2008.

[7] M. K. Varanasi and B. Aazhang, “Parametric generalized Gaussian density estimation”, *J. Acoust. Soc. Am.*, vol. 86, pp. 1404-1415, Jun. 1989.

[8] S. M. Kay, Fundamentals of statistical signal processing: detection theory, vol. II, New Jersey: Prentice Hall PTR, 1993-1998.

[9] S. Nadarajah, “A generalized normal distribution”, *J. Applied Stat.*, vol. 32, no. 7, pp. 685-694, Sep. 2005.

[10] R. Prasad, H. Saruwatari and K. Shikano, “Estimation of shape parameter of GGD function by negentropy matching”, *Neural Process. Lett.*, vol. 22, pp. 377-389, Dec. 2005.

[11] N. C. Beaulieu and Q. Guo, "Novel estimator for the location parameter of the generalized Gaussian distribution", *IEEE Commun. Lett.*, vol. 16, no. 12, pp. 2064-2067, Dec. 2012.

[12] N. C. Beaulieu and Q. Guo, "True ML estimator for the location parameter of the generalized Gaussian distribution with p = 4", *IEEE Commun. Lett.*, vol. 17, no. 1, pp. 155-157, Jan. 2013.

[13] Q. Guo and N. C. Beaulieu, "An approximate ML estimator for the location parameter of the generalized Gaussian distribution with $p = 5$", *IEEE Signal Process. Lett.*, vol. 20, no. 7, pp. 677-680, Jul. 2013.

[14] A. D. Poularikas, Transform and applications handbook, 3rd ed., Boca Raton, Florida: CRC Press, 2011.

[15] S. Kotz, T. J. Kozubowski and K. Podgórski, The Laplace distribution and generalizations: a revisit with applications to communications, economics, engineering, and finance, Boston: Birkhäuser, 2001.

[16] Mood, Graybill and Boes, Introduction to the theory of statistics, 3rd ed., New York: McGraw-Hill, 1974.

[17] A. M. Mineo and M. Ruggieri, "A software tool for the exponential power distribution: the normalp package", *J. Stat. Softw.*, vol. 12, no. 4, Jan. 2005.

[18] S. M. Kay, Fundamentals of statistical signal processing: detection theory, vol. I, New Jersey: Prentice Hall PTR, 1993.

[19] R. S. Irving, Integers, polynomials, and rings: a course in algebra, New York: Springer, Dec. 2003.

[20] F. W. J. Olver, D. W. Lozier, R. F. Boisvert and C. W. Clark, NIST handbook of mathematical functions, Cambridge, UK: Cambridge University Press, 2010.

[21] E. L. Lehmann and G. Casella, Theory of point estimation, New York: Springer, 1998.

[22] K. Lange, Numerical analysis for statisticians, New York: Springer, 1999.

[23] P. J. Huber, Robust statistics, 2nd ed., Hoboken, New Jersey: Wiley, 2009.

[24] J. Zhang, "A highly efficient L-estimator for the location parameter of the Cauchy distribution", *Comput. Stat.*, vol. 25, no. 1, pp. 97-105, 2010.

[25] N. C. Beaulieu, and C. Leung, "On the performance of three suboptimum detection schemes for binary signaling", *IEEE Trans. Commun.*, vol. 33, no. 3, pp. 241-245, Mar. 1985.

[26] A. Papoulis and S. U. Pillai, Probability, random variables and stochastic processes, 4th ed., New York: McGraw-Hill, 2002.

[27] S. Jiang and N. C. Beaulieu, "Precise BER computation for binary data detection in bandlimited white Laplace noise", *IEEE Trans. Commun.*, vol. 59, no. 6, pp. 1570-1579, Jun. 2011.

[28] R. J. Marks, G. L. Wise, D. G. Haldeman and J. L. Whited, "Detection in Laplace noise", *IEEE Trans. Aerosp. Electron. Syst.*, vol. AES-14, no. 6, Nov. 1978.

[29] M. Rosenblatt, "A central limit theorem and a strong mixing condition", *Proc. Nat. Acad. Sci.*, vol. 42, no. 1, pp. 42-47, 1956.

[30] N. C. Beaulieu, "On the performance of digital detectors with dependent samples", *IEEE Trans. Commun.*, vol. 36, no. 11, pp. 1248-1254, Nov. 1988.

[31] J. R. Barry, E. A. Lee and D. G. Messerschmitt, Digital communication, 3rd ed., New York: Springer, 2003.

[32] R. L. Graham, D. E. Knuth and O. Patashnik, Concrete mathematics: a foundation for computer science, 2nd ed. Reading, Mass.: Addison-Wesley, 1994.

[33] S. Banerjee and M. Agrawal, "Underwater acoustic noise with generalized Gaussian statistics: effects on error performance", *OCEANS-Bergen, IEEE MTS/IEEE*, pp. 1-8, Jun. 2013.

Appendix A

Asymptotic performance analysis of an optimal detector in generalized Gaussian noise

A.1 Derivation of Eqs. (3.34 - 3.36)

The derivation of Eqs. (3.34 - 3.36) are given as following.

$$\int_{-\infty}^{-\mu} \left(\frac{x-\mu}{\alpha}\right)^k \frac{1}{2\Gamma(1+1/p)\alpha} \exp\left\{-\left(\frac{|x-\mu|}{\alpha}\right)^p\right\} \mathrm{d}x$$

$$= \int_{-\infty}^{-\frac{2\mu}{\alpha}} z^k \frac{1}{2\Gamma(1+1/p)} \exp(-|z|^p) \mathrm{d}z$$

$$= \int_{\frac{2\mu}{\alpha}}^{\infty} (-1)^k t^k \frac{1}{2\Gamma(1+1/p)} \exp(-t^p) \mathrm{d}t$$

$$= \frac{(-1)^k}{2\Gamma(1+1/p)} \int_{(\frac{2\mu}{\alpha})^p}^{\infty} \frac{s^{\frac{k+1}{p}-1} \exp(-s)}{p} \mathrm{d}s$$

$$= \frac{(-1)^k}{2\Gamma(1/p)} \Gamma\left[\left(\frac{k+1}{p}\right), \left(\frac{2\mu}{\alpha}\right)^p\right] \tag{3.34}$$

$$\int_{\mu}^{\infty}\left(\frac{x-\mu}{\alpha}\right)^k\frac{1}{2\Gamma(1+1/p)\alpha}\exp\left\{-\left(\frac{|x-\mu|}{\alpha}\right)^p\right\}\mathrm{d}x$$

$$=\frac{1}{2\Gamma(1+1/p)}\int_0^{\infty}z^k\exp(-|z|^p)\mathrm{d}z$$

$$=\frac{1}{2\Gamma(1+1/p)}\frac{1}{p}\Gamma\left(\frac{k+1}{p}\right)$$

$$=\frac{1}{2\Gamma(1/p)}\Gamma\left(\frac{k+1}{p}\right) \tag{3.35}$$

$$\int_{-\mu}^{\mu}\left(\frac{x-\mu}{\alpha}\right)^k\frac{1}{2\Gamma(1+1/p)\alpha}\exp\left\{-\left(\frac{|x-\mu|}{\alpha}\right)^p\right\}\mathrm{d}x$$

$$=\frac{1}{2\Gamma(1+1/p)}\int_{-\frac{2\mu}{\alpha}}^{0}z^k\exp(-|z|^p)\mathrm{d}z$$

$$=\frac{1}{2\Gamma(1+1/p)}\left[\int_{-\infty}^{0}z^k\exp(-|z|^p)\mathrm{d}z-\int_{-\infty}^{-\frac{2\mu}{\alpha}}z^k\exp(-|z|^p)\mathrm{d}z\right]$$

$$=\frac{(-1)^k}{2\Gamma(1/p)}\left\{\Gamma\left(\frac{k+1}{p}\right)-\Gamma\left[\left(\frac{k+1}{p}\right),\left(\frac{2\mu}{\alpha}\right)^p\right]\right\} \tag{3.36}$$

where $\mu > 0$ and $\alpha > 0$.